UC Berkeley

Title

Finite Element Analysis of Two-Dimensional Stress Time-Dependent Problems

Permalink

https://escholarship.org/uc/item/23b4q6t8

Author

King, Ian

Publication Date

1965

FINITE ELEMENT ANALYSIS
OF TWO-DIMENSIONAL
TIME-DEPENDENT
STRESS PROBLEMS

BY

IAN P. KING

FINITE ELEMENT ANALYSIS OF TWO-DIMENSIONAL

TIME DEPENDENT STRESS PROBLEMS

by

Ian P. King

Faculty Investigators: Ray W. Clough

Jerome M. Raphael

University of California
Berkeley, California

January 1965

TABLE OF CONTENTS

I

INTRODUCTION

Recent advances in science and engineering have demanded more satis-
factory methods of analysis of continuous systems. Problems with irregular
configurations and boundary conditions have always been of particular
interest. Solutions in the form of complex integral or differential
equations are no longer acceptable to engineers. The designers of space
vehicle components or very high dams need realistic numbers on which to
make their decisions.

The last ten years have brought the rapid development of the auto-
matic digital computers resulting in machines that have an increasingly
effective capacity to handle large problems.

It is difficult to solve the partial differential equations that
define two dimensional stress problems. When restriction is made to the
linear elastic case, certain problems of a simple nature may be explicitly
solved and others formulated in such a way that it is possible to inter-
pret the form of solution. The vast mass of general problems with arbi-
trary boundary conditions and loading remain unsolved by exact methods.

By its very nature, the digital computer is not well suited to
solving partial differential equations; it is, however, very effective
in solution of simultaneous linear equations. Solution techniques that
adapt the two dimensional stress equations to this form have aroused
much attention recently.

The well-known finite difference method is applicable to the
solution of such problems and has, in fact, been used on several linear

elastic problems by Zienkiewicz.[1]* These cases were previously considered insoluble. The analyses concerned, however, were treated as special cases, and no general solution was attempted. The finite difference method has several inherent problems. Real boundary conditions are hard to satisfy if a rectangular net is used, and are impossibly complex if any other net is developed. The biharmonic equation requires points outside of the boundary if central differences are used, and other difference methods yield unreliable answers because of the varying order of the error term. The matrix relating the external forces and displacements does not have any guarantee of being positive definite nor, indeed, does it always have symmetry. The Gauss-Seidel interative procedure does not guarantee convergence, and direct solution methods are more likely to be sensitive. Then solution for very large problems may be very difficult to achieve without sophisticated error-correcting techniques. Finally, for problems involving non-uniform media, it is difficult to specify the linking equations. It is principally because of the problems in boundary conditions and solution that no general linear elastic two dimensional stress computer programs are available.

A separate method of attack is commonly called the "Finite Element Method." In this procedure, which is in principle applicable to all classes of continuum problems, the system is physically approximated by an assemblage of elements connected at only a finite number of points. For the two-dimensional stress problem, the elements chosen have been either one or two dimensional.

*Superscripts refer to Bibliography at the end of the text.

Hrennikoff[2] and McHenry[3] have used one dimensional elements. They assumed an assemblage of bars capable of taking axial forces combined in a rectangular element. The properties of the bars were selected to give load deflection characteristics for the element which corresponded to the plate section represented. The procedure was, however, limited to a Poisson's ratio of one-third. A later development by McCormick[4] has used a more complex form of bars where bending was allowed. This removed the restriction on Poisson's ratio. The nature of the rectangular elements leads to the same restriction on accuracy at the boundary as for the finite difference procedure.

A more recent approach has been to use a two dimensional element as the basic form. Clough[5] developed a procedure for both the rectangular and triangular elements, connected only at the corners. The triangular elements provide a good fit of boundaries and realization of the boundary conditions.

Because the finite element procedure for the two-dimensional element uses the stress-strain relationship as part of its direct formulation, it is applicable to certain non-linear problems. Techniques that use step by step methods or successive approximations have been described by Wilson[6] who also reformulated the triangular element with a physical interpretation of its mechanism.

It has long been known that many materials have properties that are dependent on time, and that any analysis which neglects this effect will have some degree of error. Concrete is an example of such a material, it exhibits a very strong dependence upon time. There have

been very few successful attempts to predict the behavior of such materials. Most experimental results have only been obtained from one dimensional tests. There has been no completely satisfactory physical explanation of creep in concrete; indeed, the results show that creep in concrete may be different from similar deformations in metals.

SCOPE

This dissertation will be concerned with the solution of generalized plane stress or plane strain problems which have time-dependent material properties. The finite element method will be used in this analysis. It will be assumed that materials have an initial elastic response followed by a creep strain which is dependent upon stress level and time.

In the derivation of the effect of creep, it will be assumed that the directions of the principal stresses are approximately invariant over an interval, and that the creep model for one direction can be expanded into two dimension along these directions. A second approach, which will not be pursued, would be to derive the creep effects from time dependent shear and bulk modulus.

In order to make a sample analysis, recently proposed creep equations for concrete will be discussed, and a final equation will be selected for use.

The derivation of elastic influence coefficients for an infinite half plate will be presented. These make possible

analysis of problems that are assumed to be supported on elastic foundations.

The computer program developed for the complete analysis will be briefly described, and the procedures for automating input and output for the computer will be outlined. These methods involve the use of subsiduary plotting equipment with programs used on the main computer to generate magnetic tapes for these plotters.

Finally, the analysis of two examples will be described. A concrete gravity dam will illustrate the application to problems meaningful to the engineering profession. In this analysis, the construction sequence is traced. The effect of thermal stresses and the changing geometry of the system are incorporated. A second example will be used to demonstrate the use of automatic plotting techniques for evaluation of results. It will demonstrate that creep effects at an early age can be significant in the reduction of stress level.

II

THE FINITE ELEMENT METHOD FOR TWO-DIMENSIONAL STRESS SYSTEMS

This chapter will outline the finite element approach to two-dimensional stress analysis, and will point out salient factors that will be relevant in later discussion of the time-dependent problem.

Fig. 1a shows a typical two-dimensional stress problem, a plate subjected to in-plane loading. Fig. 1b shows a finite element representation of the plate and its load. The continuous area of the plate has been cut into a series of triangular elements. These elements are assumed to be joined by pins at their vertices. The continuous stress problem is thus reduced to one of finite size, because a force displacement relationship can be written for each triangle. This problem is directly soluble by structural analysis techniques. The equations are linear in form. There will be only two unknowns at each joint, and one element will thus be associated with six displacement degrees of freedom.

In order to maintain displacement compatibility for the complete system, the force displacement relationship for each triangular element must be so constrained that the deflected shape of each side remains a straight line. This restriction is satisfied when the horizontal, vertical and shear stresses are forced to be constant over the whole area of the element. This may be demonstrated to be correct by consideration of what a straight line deflected shape implies. The derivative of a straight line is a constant, therefore, the strains over an element will be constant in any given direction.
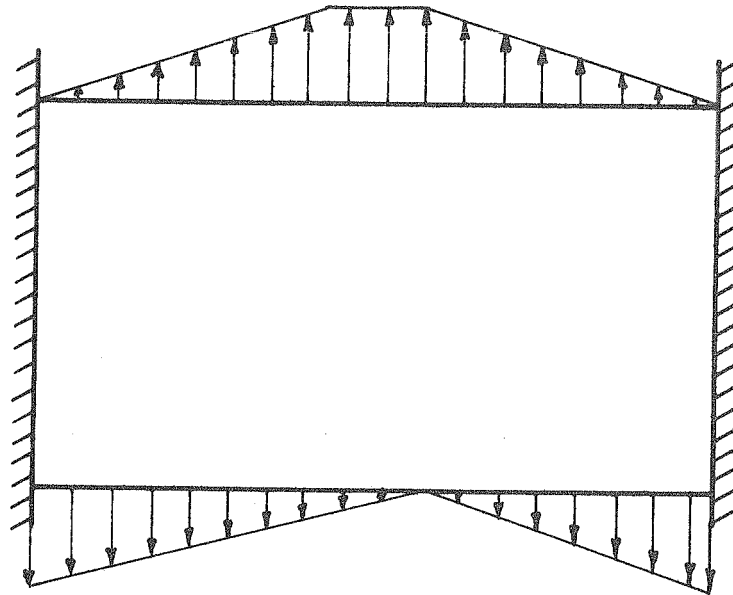
Fig. 1a   TYPICAL PLATE   WITH   IN-PLANE   LOADING
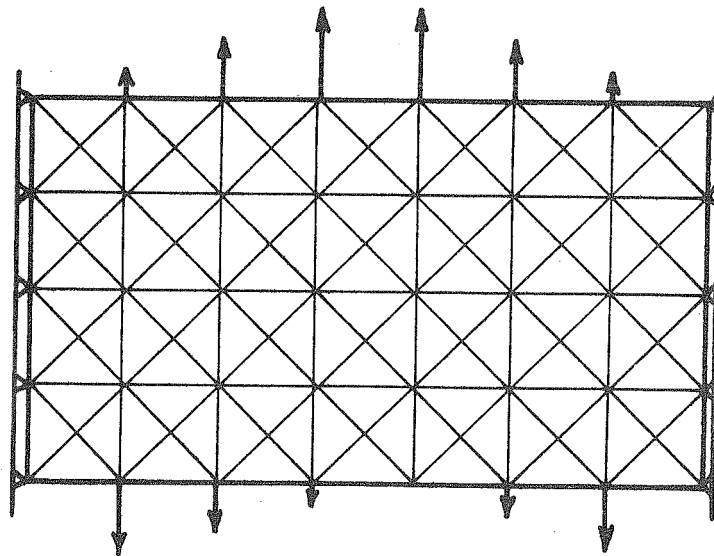

Fig. 1b   TYPICAL PLATE   WITH   FINITE ELEMENT
           REPRESENTATION   AND   LOADING

The linear isotropic stress-strain relationship results in constant

stress if constant strain exists.

Well established methods of matrix analysis may be used to

derive the force deflection relationship. The procedure described

below is more fully described by Wilson.[6]

The displacement transformation matrix $[A]$ relating corner or

nodal displacements to strains may be written as

$$[\epsilon] = [A][r] \qquad\qquad \text{II-1}$$

where $[r]$ is the column vector of the six corner displacements and

$[\epsilon]$ is the column vector of the three strain components.

The linear isotropic stress strain relationship $[S]$ for the

two-dimensional stress problem may be applied to derive the three

components of stress $[\sigma]$.

i.e.,

$$[\sigma] = [S][\epsilon] \qquad\qquad \text{II-2}$$

where

$$[S] = \frac{E}{(1+\eth)(1-2\eth)} \begin{bmatrix} 1-\eth & \eth & 0 \\ \eth & 1-\eth & 0 \\ 0 & 0 & \frac{1-2\eth}{2} \end{bmatrix}$$

The forces at the corners can be considered as the stress

resultants of the triangle and so by simple statics it is possible

to write the force transformation matrix $[B]$ from stresses to

forces. When $[R]$ represents the column vector of nodal forces

$$[R] = [B][\sigma] \qquad\qquad \text{II-3}$$

Then combining equations II-1, II-2, and II-3 to eliminate $[\epsilon]$ and $[\sigma]$

$$[R] = [B][S][A][r] \qquad\qquad \text{II-4}$$

or $$[R] = [k][r] \qquad\qquad \text{II-5}$$

where $[k]$ is the triangular element stiffness matrix which relates external or stress resultant forces to external or nodal displacements. By virtual work principles it may be shown that

$$[B] = [A]^\mathsf{T}$$

The complete stiffness of the system may then be obtained by the use of the "direct stiffness procedure." In this method, the element stiffness matrices are superposed into the total stiffness matrix. The internal coordinate system is matched to the external system to locate individual elements.

The total stiffness equation may be written as

$$[R_t] = [K][r_t] \qquad\qquad \text{II-6}$$

where $[R_t]$ and $[r_t]$ are the column vectors of all external forces and displacements and $[K]$ is the total stiffness matrix of the system.

Conventional solution of simultaneous equations leads directly to the solution for the nodal displacements of the system, and then

$$[r_t] = [K]^{-1}[R] \qquad\qquad \text{II-7}$$

The displacement transformation matrix $[A]$ from II-1 may now be used to determine element strains. This matrix acts on the submatrices $[r]$ formed from $[r_t]$ for each element. This latter process is the reverse procedure to the formation of the total stiffness matrix. The stress strain relationship II-2 then gives the element stresses from these strains, i.e.

$$\begin{bmatrix} \sigma \end{bmatrix} = \begin{bmatrix} S \end{bmatrix} \begin{bmatrix} A \end{bmatrix} \begin{bmatrix} v \end{bmatrix} \qquad \text{II-8}$$

A value for the coordinate stresses may be obtained by this transformation.

The finite element method thus discretizes the continuous form into an approximate but finite system. It then solves this approximate system exactly. The satisfactory application of this procedure is dependent upon the maintenance of compatibility of displacements along the element boundary. It is possible to show that the solution obtained is a lower bound to the exact solution in an energy sense.[7]

Forces between elements are transmitted by the stress resultants at each nodal point. Although equilibrium in the continuum is not fully satisfied, these forces are in equilibrium with each other when the system is analyzed. The stresses over the element are, of course, in equilibrium with the nodal forces. The equilibrium conditions within each element are exactly satisfied.

III

<u>THE APPLICATION OF THE FINITE ELEMENT PROCEDURE TO PROBLEMS IN</u>

<u>LINEAR VISCO-ELASTICITY</u>

The use of time dependent material properties adds a third

dimension -time- to the conventional elastic solution for a two-

dimensional system. In this dimension, coupling is from past into

present time only. If the total stress and strain history is known

at an instant of time t, then it is possible to proceed by an infin-

itesimal increment δt to a new state. The strains are held constant

for this interval, and then an instantaneous relaxation of the

accumulated stress occurs. The system then returns to an equilibrium

configuration at a time t + δt.

A numerical solution to this type of problem demands a finite

time interval Δt which can be made small enough for the solution

obtained to converge on the exact solution.

The stresses of the system are time dependent, they will change

during the interval of time Δt. The new stress system will not give

complete equilibrium of forces at a joint. These unbalanced forces

may be relaxed out by a complete elastic solution applied at the end

of the time interval. This is the relaxation referred to when

describing the infinitesimal increment.

In the application of the finite element procedure to this

problem, the structure is assumed to be maintained in its displaced

position during the time interval Δt. The nodal points are, there-

fore, also in a fixed position. The stresses are assumed to change

in each element according to the prescribed creep equation. In

general, these changes will be dependent on the whole stress

history of the element. All the changes of stress that occur will

be subjected to the same restraints as the original element

stresses that were developed by the finite element method for

elastic analysis. That is, each element must have a constant

stress distribution over its entire area.

The calculation of the stress changes of the restrained

triangular element is equivalent to finding the reduction of stress

due to relaxation of the one dimensional element.

To use the finite element procedure, the stress changes must

be converted to nodal point resultant forces. The summation of

these forces for each nodal point, taking all the elements connected

to it, will form the pseudo-external loads.

Let the total stress distribution at the end of a time interval

of relaxation by given by σ_1 and σ_2. σ_1 and σ_2 are the principal

stresses acting at an angle θ with the horizontal axis, as shown

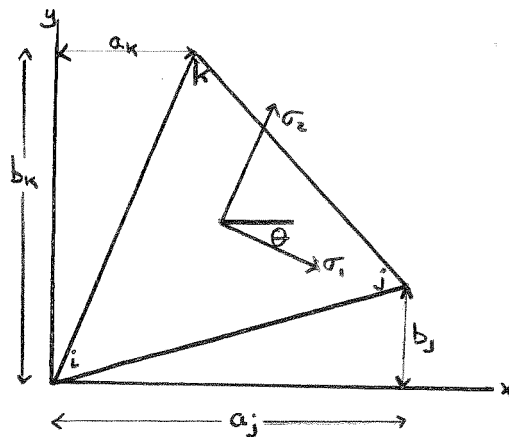in Fig. 2. The element dimensions are also shown.

Fig. 2. Triangular Element Dimensions

The transformation of principal stresses to coordinate stresses for each element may be represented by the matrix equation.

$$\begin{bmatrix} \sigma_x \\ \sigma_y \\ \tau_{xy} \end{bmatrix} = \begin{bmatrix} \cos^2\theta & \sin^2\theta \\ \sin^2\theta & \cos^2\theta \\ \tfrac{1}{2}\sin 2\theta & -\tfrac{1}{2}\sin 2\theta \end{bmatrix} \begin{bmatrix} \sigma_1 \\ \sigma_2 \end{bmatrix}$$

$$\begin{bmatrix} \sigma \end{bmatrix} = \begin{bmatrix} t \end{bmatrix} \begin{bmatrix} \sigma_p \end{bmatrix} \qquad\qquad \text{III-1}$$

As previously stated, the corner forces $\begin{bmatrix} R \end{bmatrix}$ resulting from the elements are, in fact, the stress resultants.

Fig. 3 shows an element in a state of uniform stress σ_x . The external forces act at the nodes i, j, k, and are in a state of static equilibrium. These forces may then be obtained by examination of the system and by the use of statics.
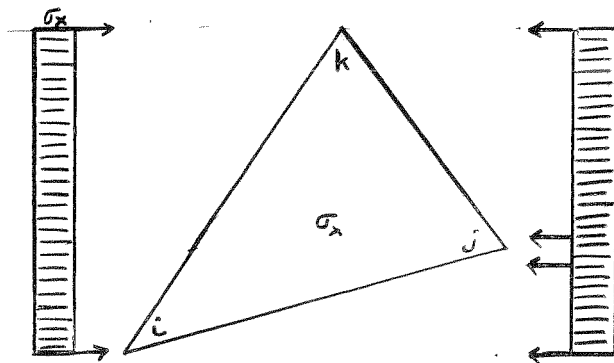

Fig. 3. Horizontal Stress Resultants

Thus at k there will be horizontal forces of 1/2 $b_k \sigma_x$ and -1/2 $(b_k - b_j)\,\sigma_x$

at j there will be horizontal forces of -1/2 $b_j \sigma_x$ and -1/2 $(b_k - b_j)\,\sigma_x$

and at i there will be horizontal forces of 1/2 $b_k \sigma_x$ and -1/2 $. b_j . \sigma_x$

The resultant forces are then equal and opposite in sign to these forces. Similar processes may be used for σ_y and τ_{xy}. In the case of σ_y only vertical forces are generated and in the equations for τ_{xy} both vertical and horizontal forces are created. A matrix form may be given to these equations.

$$
\begin{bmatrix} X_i \\ Y_i \\ X_j \\ Y_j \\ X_k \\ Y_k \end{bmatrix}
= \frac{1}{2}
\begin{bmatrix}
b_j - b_k & 0 & a_k - a_j \\
0 & a_k - a_j & b_j - b_k \\
b_k & 0 & -a_k \\
0 & -a_k & b_k \\
-b_j & 0 & a_j \\
0 & a_j & -b_j
\end{bmatrix}
\begin{bmatrix} \sigma_x \\ \sigma_y \\ \tau_{xy} \end{bmatrix}
$$

This is, in fact, the force transformation relationship previously written as

$$
\begin{bmatrix} R \end{bmatrix} = \begin{bmatrix} B \end{bmatrix} \begin{bmatrix} \sigma \end{bmatrix} \qquad\qquad \text{II-3 bis}
$$

Equations III-1 and II-3 may be combined to eliminate $\begin{bmatrix} \sigma \end{bmatrix}$, and the corner forces $\begin{bmatrix} R \end{bmatrix}$ may be obtained directly in terms of the principal stresses $\begin{bmatrix} \sigma_p \end{bmatrix}$ by

$$
\begin{bmatrix} R \end{bmatrix} = \begin{bmatrix} B \end{bmatrix} \begin{bmatrix} t \end{bmatrix} \begin{bmatrix} \sigma_p \end{bmatrix} \qquad\qquad \text{III-2}
$$

Equation III-2 may be written in full as

$$
\begin{bmatrix} X_i \\ Y_i \\ X_j \\ Y_j \\ X_k \\ Y_k \end{bmatrix}
=
\begin{bmatrix}
(b_j - b_k)\cos^2\theta + \tfrac{1}{2}(a_k - a_j)\sin 2\theta & (b_j - b_k)\sin^2\theta - \tfrac{1}{2}(a_k - a_j)\sin 2\theta \\
(a_k - a_j)\sin^2\theta + \tfrac{1}{2}(b_j - b_k)\sin 2\theta & (a_k - a_j)\cos^2\theta - \tfrac{1}{2}(b_j - b_k)\sin 2\theta \\
b_k \cos^2\theta - \tfrac{1}{2}a_k \sin 2\theta & b_k \sin^2\theta + \tfrac{1}{2}a_k \sin 2\theta \\
-a_k \sin^2\theta + \tfrac{1}{2}b_k \sin 2\theta & -a_k \cos^2\theta - \tfrac{1}{2}b_k \sin 2\theta \\
-b_j \cos^2\theta + \tfrac{1}{2}a_j \sin 2\theta & -b_j \sin^2\theta - \tfrac{1}{2}a_j \sin 2\theta \\
a_j \sin^2\theta - \tfrac{1}{2}b_j \sin 2\theta & a_j \cos^2\theta + \tfrac{1}{2}b_j \sin 2\theta
\end{bmatrix}
\begin{bmatrix} \sigma_1 \\ \sigma_2 \end{bmatrix}
$$

If the external loading is itself time dependent, the change

in the loads that occur over the interval Δt must be added to the

pseudo-external loads. This complete load system will then be

applied at the end of this interval to the entire structure. The

material properties taken are those at the instant at which the

analysis is to be made. The analysis is purely elastic; the

resulting stresses are superimposed upon the residual distribution

that existed at the time of this relaxation. A new stress state

may then be used to repeat the process for a succeeding interval

of time Δt.

The system is in equilibrium with the external loads as the

result of this addition of stresses. Let the total unbalanced

forces on the complete system at the end of a time interval be

given by a vector dF, and the change in the external loading by

a vector dR. The applied load will be the sum of these two

vectors, dF + dR.

The residual stress state will be in equilibrium with R-dF.

The stresses obtained from an elastic solution for the load of

dF + dR plus the residual stresses in the system will then be in

equilibrium with an external load system given by

$$(R - dF) + (dF + dR) = R + dR$$

which is, in fact, the external load at the end of the time

interval.

Most experimental results have led to models for the visco-

elastic response which are essentially one-dimensional in form.

It will be assumed that direct expansion into the two-dimensional

form is possible when the models are allowed to act along the

principal directions.

In order to make a sample analysis, a definite form must be

given to the relaxation function. It is also necessary to make

restrictions upon the form of these functions so as to make

possible a complete analysis within a reasonable time on the

digital computer. The same restriction will allow a satisfactory

number of elements to be used in the solution. The restriction

will be to say that the model used must allow expression of all

its previous history in the time derivatives at the time of

interest. It is preferable that they be carried in the first few

derivatives. This may be called a restriction of the Markov type.

In chapters V, VI, VIII, and IX of this dissertation, it is

assumed that the strain is a linear function of stress level. This

is not a necessary condition, and Appendix I will demonstrate a

derivation of a non-linear case.

Concrete will be taken as the material for which the creep effects will be studied. The next chapter will be devoted to the selection of an appropriate model. The derivation of the relaxation function for the selected model will follow.

IV

SELECTION AND APPLICATION OF A MODEL FOR CREEP IN CONCRETE

For greater simplicity in application to the finite element

procedure, the desired viscoelastic function should be a relaxation

model. Experimental data on relaxation in concrete are rarely

obtained as most data are based upon one dimensional creep tests

where the material is strained under a constant stress. Therefore,

a model will be selected which fits this form of data. Many models

have been proposed for the creep function of concrete. Most have

no rational basis, but are aimed at fitting the experimental data

empirically.

The creep function will be defined as the kernel f(t,T) of

the integral equation defining strain in terms of stress, i.e.,

$$\epsilon = \int_{t_o}^{t} f(t,T) \frac{\partial \sigma}{\partial T} \, dT \qquad\qquad \text{IV-1}$$

where t is the time at present and T is a dummy variable from t_o

to t.

For a creep test conducted at constant stress σ the total

strain ϵ is given by

$$\epsilon = \epsilon_c + \sigma/E_{(t)} \qquad\qquad \text{IV-2}$$

In this case $\sigma/E_{(t)}$ represents the total instantaneous elastic

strain at time t and ϵ_c the creep strain. Fig. 4 shows the
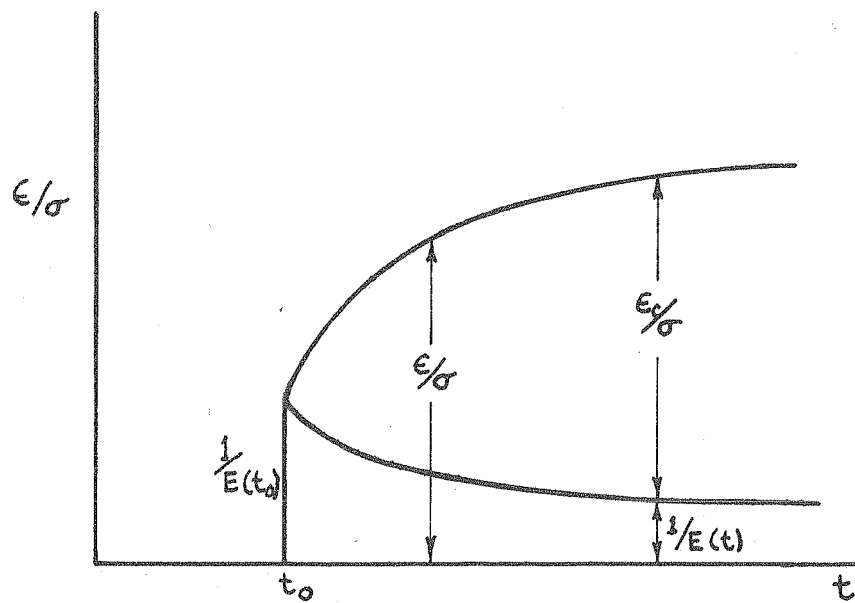
typical results of such a test.

Fig. 4   TYPICAL   CREEP   TEST   RESULTS

It is the quantity ϵ_c/σ that most investigators define as creep although some do include the $1/E_{(t)}$ term as $1/E_{(t_0)}$. This leads to difficulties when the principle of superposition is used to define the strain state upon unloading.

It is usually assumed that below one-third of the ultimate stress, the creep strain is linearly dependent upon stress level. Three forms of such linear stress dependent relationships for creep will be discussed in this chapter.

Hanson[8] in 1953 showed good numerical agreement with an equation of the form

$$\epsilon_c = \sigma \cdot a_{(T)} \, log_e \left(t + 1 - T \right) \qquad \text{IV-3}$$

where T is the time at loading, t is the present time, and a(T) is a function of T determined from empirical curve fittings of creep data. Zero time is considered to be the time at which the concrete was deposited.

In 1943, McHenry[9] proposed

$$\epsilon_c = \sigma \sum_{i=1}^{N} a_i{}_{(T)} \left(1 - e^{-m_i (t - T)} \right) \qquad \text{IV-4}$$

where he suggested that N be made sufficiently large to be certain of good agreement. $a_i (T)$ are again empirical functions of T and m_i are constants.

Hansen[10] recently proposed that a comprehensive equation of the form

$$\epsilon_c = \sigma \left(a_{(T)} \left\{ 1 - e^{-m (t - T)} \right\} + b_{(T)} \, log_e \left(t/T \right) \right) \qquad \text{IV-5}$$

In this case a(T) and b(T) were not obtained from curve fitting,

but from an appraisal of the influence of the constituents and structural form of the particular mixture of concrete.

All three equations have their particular advantages and disadvantages. The Hanson equation (IV-3) and Hansen equation (IV-5) imply that creep continues indefinitely under a constant load, although both equations reach infinity infinitely slowly. The McHenry equation (IV-4) implies a fixed maximum creep strain for a given load. It is difficult to give a definitive answer as to which is correct as there is very little test data for very long-term tests (30-50 years). The data that are available show a very definite drop from a straight line when plotted against the logarithm of time. However, for the purposes of most analyses, time beyond one year is not needed, and at this time, the difference between the curves can be made fairly small. Many more tests will be needed before a well-defined answer can be given, particularly so because the effect of drying shrinkage must be carefully investigated at the same time.

There has also been some discussion as to the validity of many of these equations when very early age (0-2 days) loadings are considered. At this time, the concrete is undergoing a rapid change of structure, and these equations may be very erroneous. This difficulty will be neglected since most practical problems do not involve loading before the concrete is two days old, indeed, it may well be necessary to include dynamic effects if such a problem were considered.

Hansen's equation was compared for the most part with results obtained from plain structural concrete with rich mixtures. It proved very difficult to get a satisfactory fit to the data for the weak mixtures typical of mass concrete. These latter mixtures, in fact, seemed to have a characteristically different form for the creep strain.

In the one degree of freedom system described by equation IV-1, a numerical solution would involve the whole stress history being traced as a succession of increments $\Delta\sigma$. It would be necessary to keep track of each increment when evaluating the total strain. Clearly for the multi-degree of freedom system represented by the finite element analysis of a two-dimensional body, this would lead to a prohibitive amount of bookkeeping.

Simplification is possible for both McHenry's equation IV-4 and Hansen's equation IV-5, because they can be expressed at any given time as rheological models. The total stress history can then be carried in the strains and rates of strains of the elements of these models. This is a Markov process. The Hanson equation IV-3 does not have a comparable representation, and it is, in fact, not possible to represent past history by the strains and rates of strain at a given time. Equation IV-3 will not be discarded in favor of the equations IV-4 and IV-5. Relaxation curves will be derived for these equations in the context of the triangular element.

It has been stated earlier that it is necessary to determine the stress as a function of time for the restrained triangular element. At the same time, the one-dimensional effect will be considered as being expandible into two dimensions by the use of the creep model along the lines of action of the principal stresses.

The stress strain relationship may be written as

$$\epsilon = \int_{t_0}^{t} f(t,T) \frac{\partial \sigma}{\partial T} dT \qquad \text{IV-1 bis}$$

or

$$\epsilon = \int_{\sigma_{t_0}}^{\sigma_t} f(t,T) d\sigma(T) \qquad \text{IV-6}$$

This second form IV-6 is amenable to a finite difference solution, for the integral may be written, when the simple rectangular summation is used as

$$\epsilon = \sum_{j=1}^{m} f(t_m, t_j) \Delta\sigma_j \qquad \text{IV-7}$$

where $\Delta\sigma_j$ represents the change in σ over an interval of time Δt where

$$\Delta t = (t_m - t_0)/m \qquad \text{IV-8}$$

For stress relaxation under a fixed initial strain, the strain remains constant for a further time interval Δt.

Therefore

$$\sum_{j=1}^{m+1} f(t_{m+1}, t_j) \Delta\sigma_j = \sum_{j=1}^{m} f(t_m, t_j) \Delta\sigma_j \qquad \text{IV-9}$$

or

$$\sum_{j=1}^{m+1} f(t_{m+1}, t_j) \Delta\sigma_j = f(t_1, t_1) \Delta\sigma_1 \qquad \text{IV-10}$$

The right hand side of this equation represents the initial elastic strain.

The quantity $\triangle \sigma_{m+1}$ may be obtained by separating the summation and writing as

$$f(t_{m+1}, t_{m+1}) \triangle \sigma_{m+1} = f(t_1, t_1) \triangle \sigma_1 - \sum_{j=1}^{m} f(t_{m+1}, t_j) \triangle \sigma_j \qquad \text{IV-11}$$

or

$$\triangle \sigma_{m+1} = \frac{f(t_1, t_1) \triangle \sigma_1 - \sum_{j=1}^{m} f(t_{m+1}, t_j) \triangle \sigma_j}{f(t_{m+1}, t_{m+1})} \qquad \text{IV-12}$$

In this equation all the $\triangle \sigma_i$ for i=1 to m are known, therefore, the stress change in the m+1 interval $\triangle t$ is determinate. The equation IV-12 illustrates the need to carry out the m summations of the $\triangle \sigma_j$ for a single time interval and clearly all the $\triangle \sigma_j$ would have to be saved for their use in the next time interval.

APPLICATION OF McHENRY'S EQUATION

The creep function f(t,T) may be defined from the equation of McHenry as

$$f(t, T) = \left\{ \sum_{i=1}^{N} a_i(T) \left(1 - e^{-m_i(t-T)} \right) + \frac{1}{E_{(t)}} \right\} \qquad \text{IV-13}$$

Then it is possible to consider this equation to have the rheological form shown in Fig. 5. However the parameters of the constituent elements are time dependent and any approach to direct solution by inversion is impossible.

For this equation the term

$$\sum_{j=1}^{m} f(t_{m+1}, t_j) \triangle \sigma_j = \sum_{j=1}^{m} \left\{ \sum_{i=1}^{N} a_i(t_j) \left(1 - e^{-m_i(t-T)} \right) + \frac{1}{E_{(t)}} \right\} \qquad \text{IV-14}$$
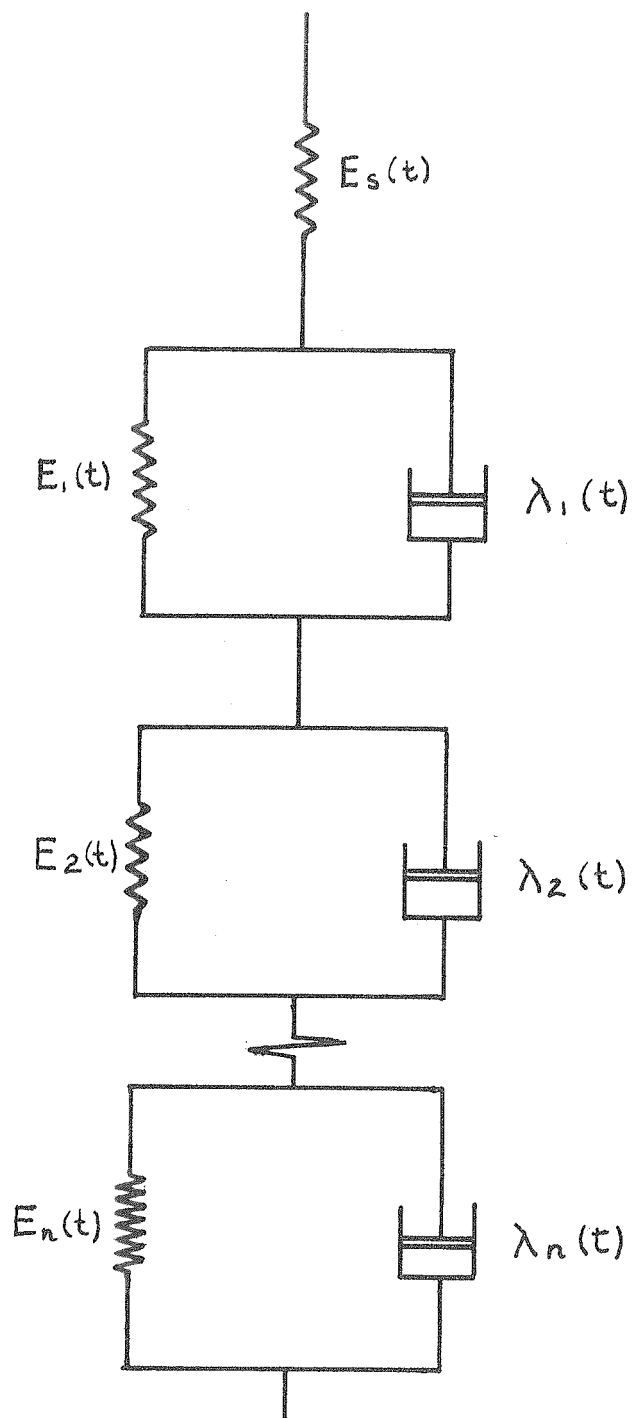
Fig. 5   SERIES   KELVIN   MODELS   FOR
Mc HENRY'S   EQUATION

or rewriting with the summations reversed

$$\sum_{j=1}^{m} f(t_{m+1}, t_j) \Delta \sigma_j = \sum_{i=1}^{N} \sum_{j=1}^{m} \left\{ a_i(t_j) \Delta \sigma_j - a_i(t_j) e^{-m_i(t_{m+1} - t_j)} \Delta \sigma_j \right\} + \sum_{j=1}^{m} \frac{\Delta \sigma_j}{E(t_{m+1})} \qquad \text{IV-15}$$

$$= \sum_{i=1}^{N} \left\{ \sum_{j=1}^{m} a_i(t_j) \Delta \sigma_j - e^{-m_i t_{m+1}} \sum_{j=1}^{m} a_i(t_j) e^{m_i t_j} \Delta \sigma_j \right\} + \frac{\sigma_m}{E(t_{m+1})} \qquad \text{IV-16}$$

Note that at the time there will be no need to do a complete sum.
For if

$$\sum_{i=1}^{N} \sum_{j=1}^{m} a_i(t_j) \Delta \sigma_j = \sum_{i=1}^{N} b_{im} \qquad \text{IV-17}$$

then $\qquad b_{im} = b_{im-1} + a_i(t_m) \Delta \sigma_m \qquad \text{IV-18}$

Similarly, if

$$\sum_{i=1}^{N} e^{-m_i t_{m+1}} \sum_{j=1}^{m} a_i(t_j) e^{m_i t_j} \Delta \sigma_j = \sum_{i=1}^{N} e^{-m_i t_{m+1}} c_{im} \qquad \text{IV-19}$$

then $\qquad c_{im} = c_{im-1} + a_i(t_m) e^{m_i t_m} \Delta \sigma_m \qquad \text{IV-20}$

IV-18 and IV-20 are direct consequences of the representation by a model
and, in fact, represent parameters of the element states at a given time.

Also

$$f(t_1, t_1) = 0 + \frac{\sigma_1}{E(t_1)} = \quad \text{initial elastic strain}$$

Then equation IV-12 may be written

$$\Delta \sigma_{m+1} = \sigma_1 \frac{E(t_{m+1})}{E(t_1)} - E_{t_{m+1}} \left\{ \sum_{i=1}^{N} b_{im} - \sum_{i=1}^{N} e^{-m_i t_{m+1}} c_{im} \right\} - \sigma_m \qquad \text{IV-21}$$

or

$$\sigma_{m+1} = \sigma_1 \frac{E(t_{m+1})}{E(t_1)} - E_{t_{m+1}} \left\{ \sum_{i=1}^{N} b_{im} - \sum_{i=1}^{N} e^{-m_i t_{m+1}} c_{im} \right\}$$

Thus, it is possible to avoid the repeated summation in obtaining the value of the stress after a given relation interval. There is no need to carry the stress history; all that is necessary is to know the values b_{im} and c_{im} for the N sets of elements.

An identical result may be obtained by physical considerations where the modification of stress is made to adjust the creep strain back to its initial value after it has been allowed to move for an interval $\triangle t$ under the creep law.

APPLICATION OF HANSEN'S EQUATION

The derivation of the relaxation function for this equation will follow the physical approach.

The equation IV-5 of Hansen may be represented as the Burgers model shown in Fig. 6. In this case, the series dashpot has a stiffness that increases linearly with time, and depends upon the time of loading. The series spring is an arbitrarily varying function of time and the parameters E_2 and λ_2 vary with the time of application of the load. Because of the irregularity of behavior, it is possible to solve this system directly only when a constant stress σ is assumed to be applied.

Simple equilibrium conditions then show that

$$\epsilon = \sigma \left\{ \frac{1}{k} \log_e t/T + \frac{1}{E_2} \left(1 - e^{-E_2/\lambda_2 (t-T)} \right) + \frac{1}{E_1} \right\} \qquad \text{IV-22}$$
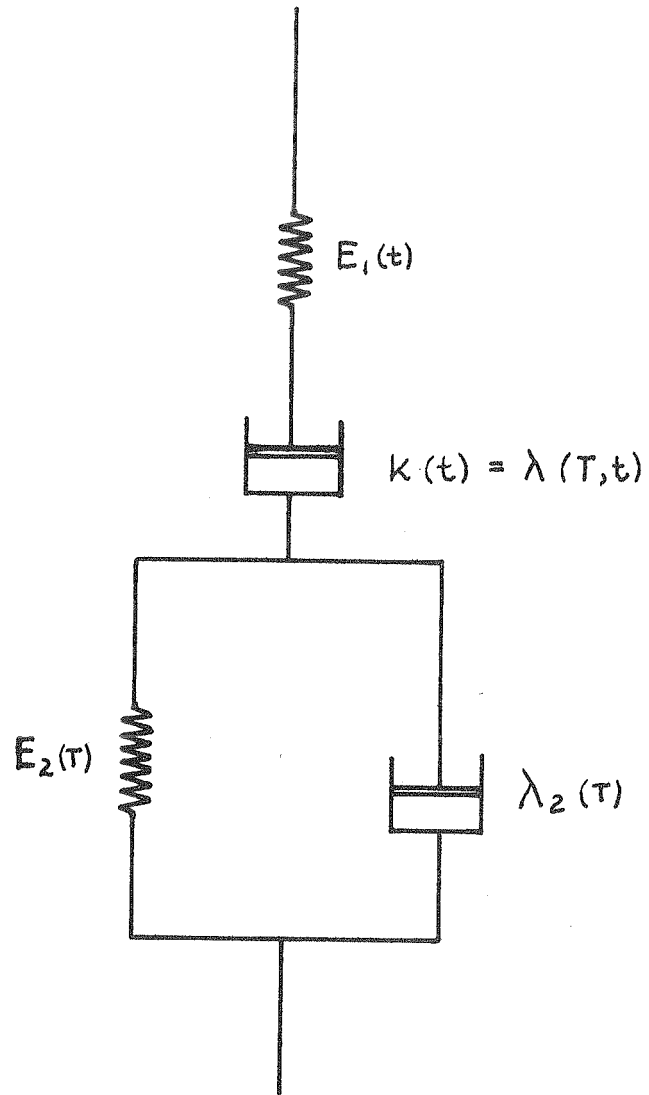
Fig. 6 BURGERS MODEL OF
HANSEN'S EQUATION

This equation then agress with Hansen's when

$$\frac{1}{E_2} = a(T) \qquad \frac{1}{k} = b(T) \qquad \frac{E_2}{\lambda_2} = m = \text{constant}$$

This is possible for any time of loading.

At constant σ

$$\frac{d\epsilon}{dt} = \sigma \left\{ \frac{1}{k} \frac{1}{t_1 T} + \frac{1}{E_2} \frac{E_2}{\lambda_2} e^{-\{E_2/\lambda_2 (t-T)\}} \right\} \qquad \text{IV-23}$$

If there have been N sudden steps of stress at equal small but finite time intervals Δt (the steps of stress being given by $\Delta \sigma_i$ for $i=1$ to N), there will be a strain in the next time interval Δt of $\Delta \epsilon$

where

$$\Delta \epsilon = \sum_{i=1}^{N} \Delta \sigma_i \left\{ \frac{1}{k_i} \frac{1}{t_N} \frac{1}{t_i} + \frac{1}{\lambda_{2i}} e^{-E_2/\lambda_{2i} t_N} e^{E_2/\lambda_{2i} t_i} \right\} \qquad \text{IV-24}$$

$$\therefore \quad \Delta \epsilon = \frac{1}{t_N} \sum_{i=1}^{N} \frac{\Delta \sigma_i}{k_i t_i} + e^{-E_2/\lambda_{2i} t_N} \sum_{i=1}^{N} \Delta \sigma_i e^{E_2/\lambda_{2i} t_i} \qquad \text{IV-25}$$

and if

$$\sum_{i=1}^{N} \frac{\Delta \sigma_i}{k_i t_i} = b_N \qquad \text{IV-26}$$

$$\sum_{i=1}^{N} \frac{\Delta \sigma_i}{\lambda_{2i}} e^{E_2/\lambda_{2i} t_i} = C_N \qquad \text{IV-27}$$

$$\Delta \epsilon = \frac{1}{t_N} b_N + e^{-E_2/\lambda_{2i} t_N} C_N \qquad \text{IV-28}$$

Then a step of stress is required to keep the strain constant; this step is

$$\Delta \sigma_{N+1} = - E_{1(t_N)} \Delta \epsilon \qquad \text{IV-29}$$

The summation

$$\sum_{i=1}^{N+1} \Delta\sigma_i = \sigma_{N+1} \qquad \text{IV-30}$$

forms the third parameter which is needed to record the stress state at the time t_{N+1} . The physical considerations thus lead to the same form of parameters as the more rigorous mathematical derivation, and it is possible to describe the stress state at the end of a given interval in terms of the conditions at the beginning of the interval. It is assumed that this interval is small enough for the solution obtained to be independent of the size of the interval within reasonable limits of accuracy. Davis and Duke[11] suggested that the theory of elasticity could be applied in expansion of one-dimensional test results to two-dimensional application. They found from tests that Poisson's ratio remained constant with time, and that superposition was a reasonable assumption.

In the finite element elastic solution of the two-dimensional problem, the principal stress directions are different for stresses due to solution of the pseudo-external load system from the direction of the principal stresses in the element residual stresses. It is, therefore, necessary to modify the creep strain parameters that have been accumulated. It will be assumed that these parameters may be treated as vectors in the principal stress directions. Fig. 7 shows the form. Then

$$b_{1N} = b_{1N} \cos d\Theta - b_{2N} \sin d\Theta \qquad \text{IV-31}$$

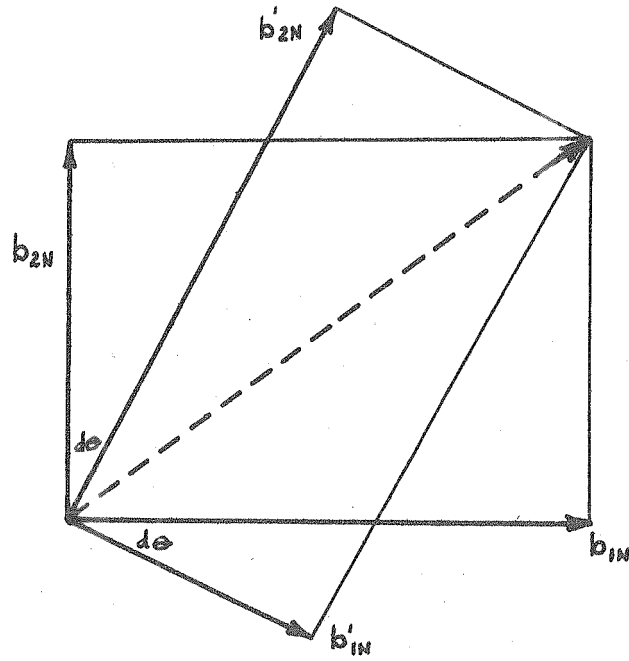$$b_{2N} = b_{1N} \sin d\Theta + b_{2N} \cos d\Theta \qquad \text{IV-32}$$

Fig. 7 CHANGE OF STRAIN PARAMETERS AS
PRINCIPAL STRESS DIRECTIONS CHANGE

The change in direction as the result of any one increment may be expected to be small, therefore the correction applied to the parameters will also be small and the effects of any error by this assumption should be negligible.

To get the most accurate solution, it would be necessary to do a complete analysis at the end of each time interval of relaxation. In the interests of practicable solution, it is necessary to allow a longer time between complete analyses. The time between complete analyses is discussed in Example I. A suitable interval for the stress relaxation is shown in the next chapter and discussed in Example II.

V

NUMERICAL COEFFICIENTS FOR THE CREEP EQUATION

Once the form of the creep equation has been decided, it is still necessary to compute the numerical coefficients. In the case of the Hansen equation, these coefficients are predetermined by the structure of the concrete. The coefficients for McHenry's equation are, however, purely empirical, and it is necessary to use a numerical curve fitting procedure.

The evaluation of coefficients for a creep equation of the form

$$\epsilon_{c(t)} = \sigma \left\{ a_1(\tau) \left(1 - e^{-m_1(t-\tau)} \right) + a_2(\tau) \left(1 - e^{-m_2(t-\tau)} \right) \right\} \qquad \text{V-1}$$

will be examined. T is the age of the concrete at loading with a constant stress σ and t is the age at the time to be considered.

Experimental data are available for deformations due to a series of single step loads. The creep may be separated from the elastic deformation by knowing the instantaneous elastic modulus at various times. A series of equations may be written for test (loaded at Ti) throughout a series of times ti.

$$\epsilon_{c_{i_1}} = \sigma_i \left\{ a_1(T_i) \left(1 - e^{-m_1(t_1 - T_i)} \right) + a_2(T_i) \left(1 - e^{-m_2(t_1 - T_i)} \right) \right\} \qquad \text{V-2a}$$

$$\epsilon_{i_2} = \sigma_i \left\{ a_1(T_i) \left(1 - e^{-m_1(t_2 - T_i)} \right) + a_2(T_i) \left(1 - e^{-m_2(t_2 - T_i)} \right) \right\} \qquad \text{V-2b}$$

$$\epsilon_{i_n} = \sigma_i \left\{ a_1(T_i) \left(1 - e^{-m_1(t_n - T_i)} \right) + a_2(T_i) \left(1 - e^{-m_2(t_n - T_i)} \right) \right\} \qquad \text{V-2c}$$

Thus, a first step is to evaluate $a_1(T_i), a_2(T_i), m_1, m_2$ for a given set of test data, for a loading at Ti.

The value of t when inserted, as in the above equations, gives an over-determined set of n non-linear equations.

These equations may be simplified if the j th point of the i th test is considered. The typical equation reduces to

$$a e^{mt} + b e^{nt} = K(t) \qquad \text{V-3}$$

where
$$t = t_j - T_i \qquad \text{V-4}$$

$$K(t) = -\epsilon_{ij}/\sigma_i + a_1(T_i) + a_2(T_i) \qquad \text{V-5}$$

and a, b, m, n, are the unknowns. The value

$$a_1(T_i) + a_2(T_i) = \epsilon_{ci\infty}/\sigma_i \qquad \text{V-6}$$

and is therefore known.

A method attributed to Prony[13] is applicable to the solution of the equation V-3. In this procedure which is restricted to data with equal increments of t, the non-linearity with respect to m and n is first eliminated and a set of linear equations for a and b obtained.

It may be proved[14] that the quadratic equation

$$u^2 - \alpha_1 u - \alpha_2 = 0$$

will give as solutions u_1, u_2 the values $e^{m \Delta t}$, $e^{n \Delta t}$ (where Δt is the prescribed data interval). The coefficients α_1 and α_2 are obtained

as the solution of the n overdetermined linear equations

$$K_{(t_1)} \alpha_1 + K_{(t_1)} \alpha_2 = K(t_2)$$

$$K_{(t_2)} \alpha_1 + K_{(t_2)} \alpha_2 = K(t_3)$$

$$K_{(t_{n-1})} \alpha_1 + K_{(t_{n-2})} \alpha_2 = K(t_n)$$

V-7

Least squares procedures may be used to determine a 'best fit' to these equations.

Then writing V-7 in matrix form

$$[K][\alpha] = [R]$$

V-8

where $[K]$ is non-square. The minimum square error for the coefficients may be found by premultiplying V-8 by $[K]^T$ and solving the resulting square set of linear equations.

That is

$$[K]^T[K][\alpha] = [K]^T[R]$$

V-9

$$[\alpha] = \left[[K]^T[K]\right]^{-1}[K][R]$$

V-10

Hence the values of u are obtained as

$$u = \alpha_1/2 \pm \tfrac{1}{2}\sqrt{\{\alpha_1^2 + 4\alpha_2\}}$$

V-11

and

$$m,n = \frac{1}{\Delta t} \log_e \tfrac{1}{2} \left\{ \alpha_1 \pm \sqrt{\{\alpha_1^2 + 4\alpha_2\}} \right\}$$

V-12

Then with m and n known, the equation V-3 may be rewritten as a set of linear equations. These equations will again be over-determined, and it is necessary to repeat the least squares operation on this set.

The complete procedure must be repeated for each set of test data for a given constant load. From all of the fitted test curves, the variation of the functions $a_1(T)$ $a_2(T)$ $m_1(T)$ $m_2(T)$ will be determined.

The creep equation of McHenry assumes that m_1 and m_2 are constants. Therefore, it is necessary to make approximations to m_1 and m_2 from the functions obtained, and then with these constant values assumed, to make a least squares analysis upon all the test data. In this case, of course, the equations are directly linear in $a_1(T)$ and $a_2(T)$.

An example of the results of such an analysis is shown in Table I where the results are compared with the input data. The agreement is clearly satisfactory.

Time	Creep obs.	Creep comp.	Error	Error percent
4.	0.3700	0.3784	0.0084	2.27
8.	0.4640	0.4723	0.0083	1.78
12.	0.5270	0.5245	-0.0025	0.48
16.	0.5750	0.5664	-0.0086	1.49
20.	0.6150	0.6026	-0.0124	2.03
24.	0.6440	0.6340	-0.0100	1.55
28.	0.6700	0.6615	-0.0085	1.27
32.	0.6880	0.6855	-0.0025	0.37
36.	0.7000	0.7064	0.0064	0.91
40.	0.7140	0.7247	0.0107	1.49
44.	0.7300	0.7406	0.0106	1.45

$$a_1 = -0.488 \qquad a_2 = -0.3628 \qquad m_1 = -0.034 \qquad m_2 = -0.52$$

Table I. Theoretical and computed coefficients for
concrete loaded at age 7 days

When Hildebrand[14] discussed the dangers of application of Prony's method, he pointed out that the results may produce an oscillatory system associated with an imaginary solution to the quadratic equation. None of the analyses made for the examples discussed in this dissertation gave this problem, but a careful watch should be kept.

Prony's method is equally applicable if N is taken to be greater than 2 in McHenry's equation IV-6. In this case, the quadratic equation becomes a polynomial equation of order N.

A stress relaxation test was simulated on the computer to check the validity of the creep function obtained using Prony's method and McHenry's equation with N equal to 2. The results were compared with experimentally obtained results for the same concrete, see Fig. 8. The agreement of the curves demonstrates the validity of the equation used and the functions obtained for the coefficients.

Finally a large set of experimental data for a series of creep tests were investigated and values for $a_1(T)$ and $a_2(T)$ obtained. A function was not easily fitted and linear interpolation had subsequently to be used. m_1 and m_2 were set at -0.034 and -0.52 respectively. These values are used in examples I and II.
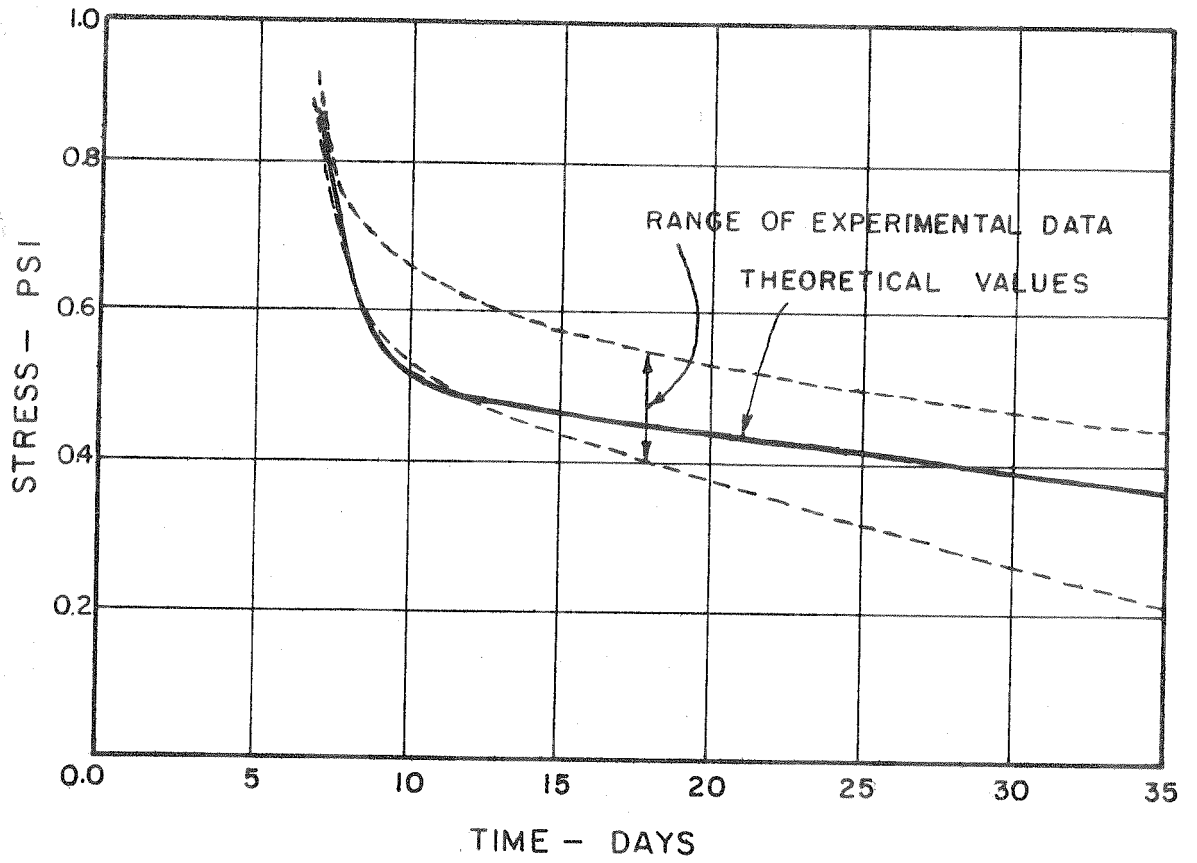
Fig. 8 RELAXATION CURVES

VI

INFLUENCE COEFFICIENTS FOR AN ELASTIC FOUNDATION

Many two-dimensional stress systems have boundary conditions that may not be satisfactorily represented by conditions of zero stress or displacement in any given coordinate directions. A large class of problems have elastic support conditions. An example of such support is the concrete gravity dam which is usually constructed on a rock foundation, as shown in Fig. 9a. For this problem, the horizontal stress at the intersection would be wrongly approximated by requiring either zero horizontal stress (i.e., no displacement restraint in the horizontal direction) or complete lateral fixity. Vertical displacements must also be allowed. Clearly, some form of flexible boundary condition is required.

The finite element method can approximate the flexibility of the foundation system by using elements constructed to cover an area of the foundation sufficiently large that simple boundary conditions may be applied to the foundation, as shown in Fig. 9b. The distance to the boundaries must be such that the stress distribution in the dam would not be varied by changing the position of the boundary a small amount away from the dam. In this case, there will be many extra elements which do not contribute significantly to the accuracy of the solution in the dam itself. It is, however, difficult to predict which, if any, elements could be removed. Solution time for the problem will be much increased. This mesh which covers the foundation does have the advantage that it is possible to handle the effects
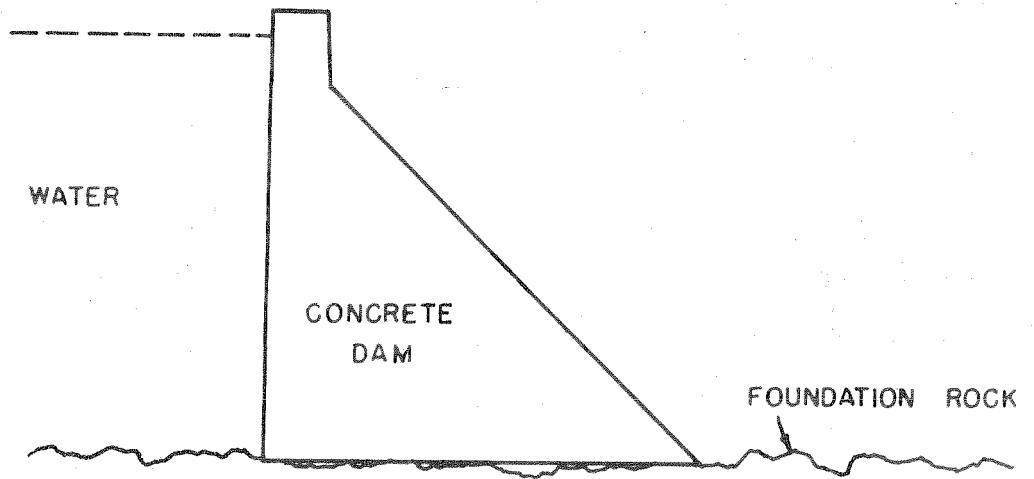
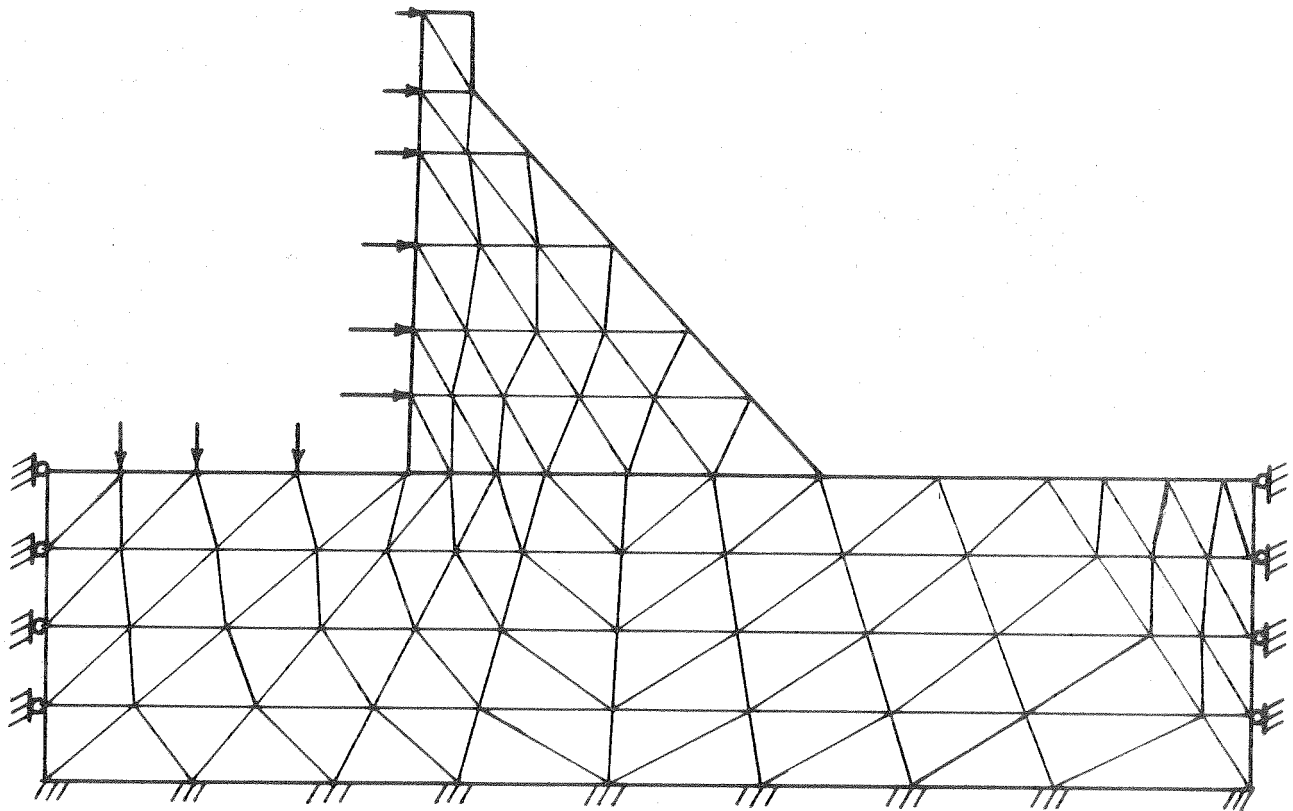Fig. 9a TYPICAL SECTION THROUGH GRAVITY DAM AND
FOUNDATION

Fig. 9b TYPICAL GRAVITY DAM AND FOUNDATION
REPRESENTED BY FINITE ELEMENTS

of non-uniform foundation media without the need to reprogram, only the element properties have to be adapted. This is particularly useful for layered rock foundations.

A different procedure is to consider the problem as that of a structural system of finite elements resting on an elastic half-plane. The nodal points of the triangular element system may then be considered as points at which the load is transmitted from the elements to the half plane, as shown in Fig. 10. Superficially, the nodal point forces may appear to be concentrated loads, but the assumptions of the finite element method imply that these forces are the stress resultants of the element interfaces. Thus, the transfer of forces may be considered as distributed over a length about equal to half the element spacing.

A method is, therefore, needed to obtain the stiffness influence coefficients for points along the surface of an elastic half-plane which has been subjected to a distributed loading in the vertical and horizontal directions.

The solution of the problem of the infinite half-plate under a distributed load is readily adapted to the solution for an infinite half-plane under conditions of plane strain. The values of the elastic moduli E and υ must be modified to become

$$E^* = \frac{E}{1-\upsilon^2} \qquad\qquad \text{VI-1}$$

$$\upsilon^* = \frac{\upsilon}{1-\upsilon} \qquad\qquad \text{VI-2}$$
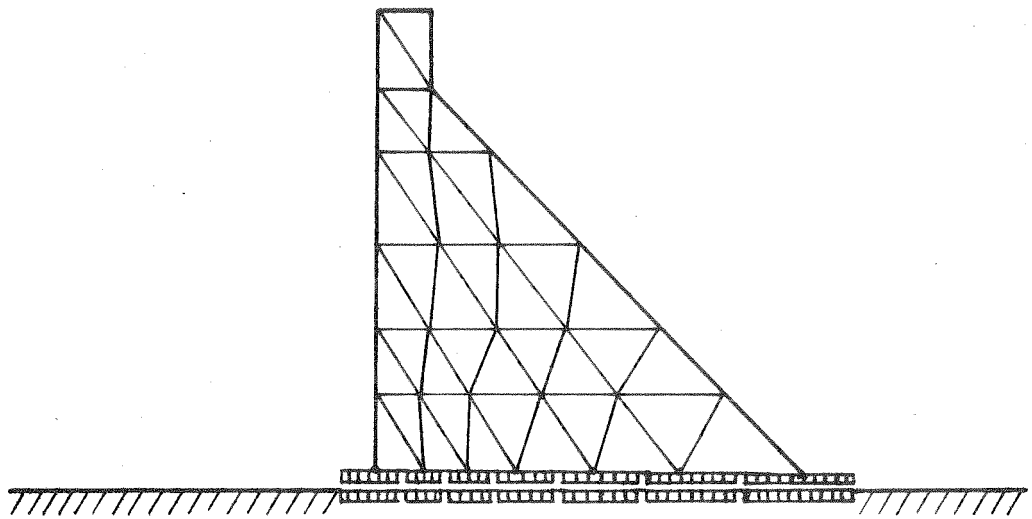
Fig. 10   TRANSMITTAL   OF   STRESS   TO

ELASTIC FOUNDATION

The stress function for the problem is well known, and integration of the equations is readily carried out,[15] for both vertical and horizontal loads.

The solution takes these forms for rectangular cartesian coordinates (see Fig. 11)

(1) For vertical loads-;

$$u = 0 \qquad\qquad x \leqslant -a \qquad \text{VI-3}$$

$$u = \frac{(1-\vartheta^*)}{E^*} q(x+a) \qquad -a \leqslant x \leqslant a \qquad \text{VI-4}$$

$$u = \frac{2(1-\vartheta^*)}{E^*} qa \qquad a \leqslant x \qquad \text{VI-5}$$

$$v = \frac{q}{\pi E^*}\left\{ (a-x)\log_e(a-x)^2 + (a+x)\log_e(a+x)^2 \right.$$
$$\left. -(a-d)\log_e(a-d) - (a+d)\log_e(a-d)^2 \right\} \qquad \text{VI-6}$$

where

$u_{(x)}$ = horizontal surface displacement at distance x from origin,

$v_{(x)}$ = vertical surface displacement at distance x from origin,

q = load per unit length

$\vartheta^* E^*$ = usual elastic moduli modified for plane strain case,

$2a$ = length of loaded line

d = distance to point at left of origin where displacements are arbitrarily set to zero.

The origin is the mid point of the load.
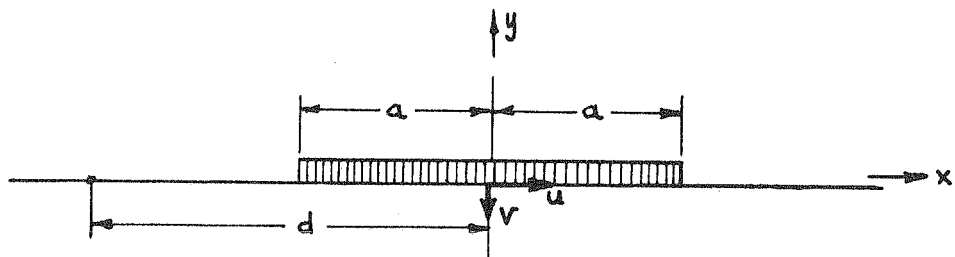
Fig. 11 DEFINITION OF COORDINATES FOR
HALF . PLATE SOLUTION

(2) For horizontal loads

$$u = \frac{q}{\pi E} \left\{ (a-x) \log_e (a-x)^2 + (a+x) \log_e (a+x)^2 \right.$$
$$\left. - (a-d) \log_e (a-d)^2 - (a+d) \log_e (a+d)^2 \right\} \qquad \text{VI-7}$$

$$v = 0 \qquad\qquad x \leqslant -a \qquad \text{VI-8}$$

$$v = \frac{(1-\nu^*)}{E^*} q (x+a) \qquad -a \leqslant x \leqslant a \qquad \text{VI-9}$$

$$v = \frac{2(1-\nu^*)}{E^*} q a \qquad a \leqslant x \qquad \text{VI-10}$$

For vertical loading, the solution apparently yields an infinite

vertical displacement in the direction of the load as the distance

from the loading tends toward infinity, similarly for the horizontal

loading, the horizontal displacement tends toward infinity. The actual

value of the displacements vary depending on the value selected for d.

The validity of these results will, therefore, be checked by compar-

ison with the solution in three-dimensional form for a half-space

subjected to a plane strain type loading.

The influence coefficients to be derived depend only on the

shape of the displacement function. Any rigid body effect that is

superimposed has no influence on the stress in the system under con-

sideration. Therefore, the solution will be satisfactory if the shape

is acceptable, without regard to its absolute size.

The vertical displacements due to a vertical uniformly distributed

load p over a rectangular area of surface of a half space have been

given by Schleicher[16].

The dimensions of the rectangular loaded area are shown in Fig. 12. The vertical displacement is given by

$$V(x,y) = \frac{1}{\pi C} \iint_{Area} \frac{P(\xi,\eta)}{(x-\xi)^2 + (y-\eta)^2} \, d\xi \, d\eta \qquad \text{VI-11}$$

where

$$C = E \Big/ (1-\vartheta^2) \qquad \text{VI-12}$$

If p is assumed to be uniform, the integration yields

$$V(x,y) = \frac{P}{\pi C} \left[\begin{array}{l} (b-y)\log_e\left(\left\{\sqrt{(a-x)^2+(b-y)^2}+(a-x)\right\}\Big/\left\{\sqrt{(a+x)^2+(b-y)^2}-(a+x)\right\}\right) \\ +(b+y)\log_e\left(\left\{\sqrt{(a-x)^2+(b+y)^2}+(a-x)\right\}\Big/\left\{\sqrt{(a+x)^2+(b+y)^2}-(a+x)\right\}\right) \\ +(a-x)\log_e\left(\left\{\sqrt{(a-x)^2+(b-y)^2}+(b-y)\right\}\Big/\left\{\sqrt{(a-x)^2+(b+y)^2}-(b+y)\right\}\right) \\ (a+x)\log_e\left(\left\{\sqrt{(a+x)^2+(b-y)^2}+(b-y)\right\}\Big/\left\{\sqrt{(a+x)^2+(b+y)^2}-(b+y)\right\}\right) \end{array} \right]$$

$$\text{VI-13}$$

The horizontal displacements may be obtained (see Appendix II) from

$$u(x,y) = \frac{1-2\vartheta}{2(1-\vartheta)} \frac{1}{\pi C} \iint_{Area} \frac{P(y-\eta)}{(x-\xi)^2 + (y-\eta)^2} \, d\xi \, d\eta \qquad \text{VI-14}$$

For uniform p this yields

$$u(x,y) = \frac{(1-2\vartheta)P}{2(1-\vartheta)\pi C} \left[\begin{array}{l} -(a-x)\tan^{-1}\left(\frac{b-y}{a-x}\right) - (b-y)\log_e\sqrt{(b-y)^2+(a-x)^2} \\ +(a+x)\tan^{-1}\left(\frac{b-y}{a+x}\right) + (b-y)\log_e\sqrt{(b-y)^2+(a+x)^2} \\ -(a-x)\tan^{-1}\left(\frac{b+y}{a-x}\right) - (b+y)\log_e\sqrt{(b+y)^2+(a-x)^2} \\ +(a+x)\tan^{-1}\left(\frac{b+y}{a+x}\right) + (b+y)\log_e\sqrt{(b-y)^2+(a+x)^2} \end{array} \right]$$
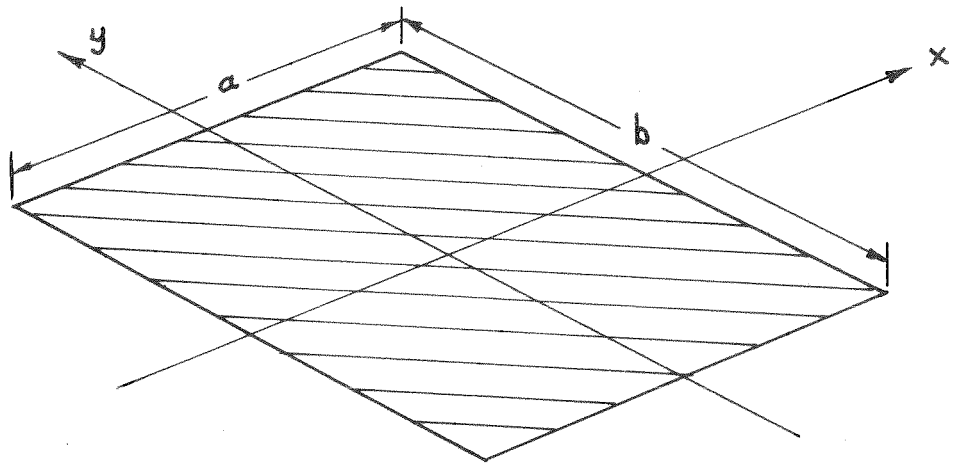
$$\text{VI-15}$$

Fig. 12 COORDINATE DIRECTIONS AND AREA OF LOAD
FOR INFINITE HALF SPACE SOLUTION

The three-dimensional problem with a long thin uniformly loaded strip approximates a plane strain problem at the center of loading, and therefore the result may be directly compared with the two-dimensional solution already given. A case was chosen where

$a = 36,000"$ $b = 100"$ $E = 5.0 \times 10^6$ p.s.i. $= 0.17$ $d = 0.$

Fig. 13 shows a plot of displacement under the loaded strip against position under the strip for the case above. The approximately constant value under the center portion of the loaded strip confirms that the loading at the center is close to one of plane strain. Fig. 14 is a plot of vertical displacement along a line in the surface normal to the strip at the center point. This is compared with a plot of the displacements obtained for the thin plate solution. The coordinates on the plot have been translated so that both solutions give the same displacement under the load. The closeness of these two lines indicates that the use of the thin plate solution is justified. The horizontal displacements for both cases are shown plotted in Fig. 15, the small difference between the results show that the agreement is again good. Fig. 14 and Fig. 15 show that the solution does not depend significantly on the location of the arbitrary zero point.

Consider the system shown in Fig. 16. A uniform load is shown applied to the plate. Because of the stress conditions on the boundary, it is necessary to provide two supports for the plate. Displacements would be infinite if the supports were not provided, that is, the flexibility matrix becomes singular. One of the supports is pinned, the other is on rollers. The supports also create reactive forces F_L and F_R as shown; these support forces are also assumed to be distributed. These forces can cause concentration effects and thus will be
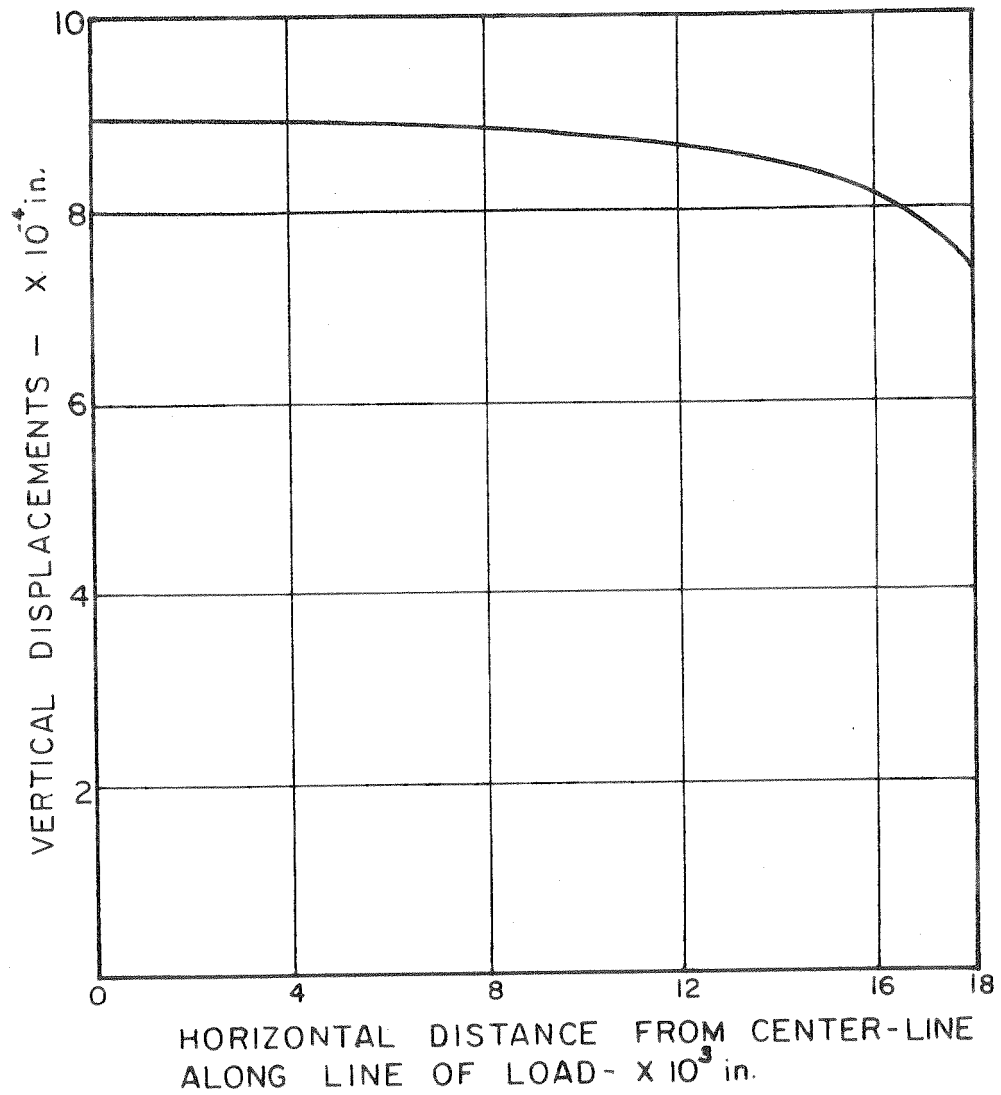
49

Fig. 13   VERTICAL DISPLACEMENTS UNDER STRIP LOAD
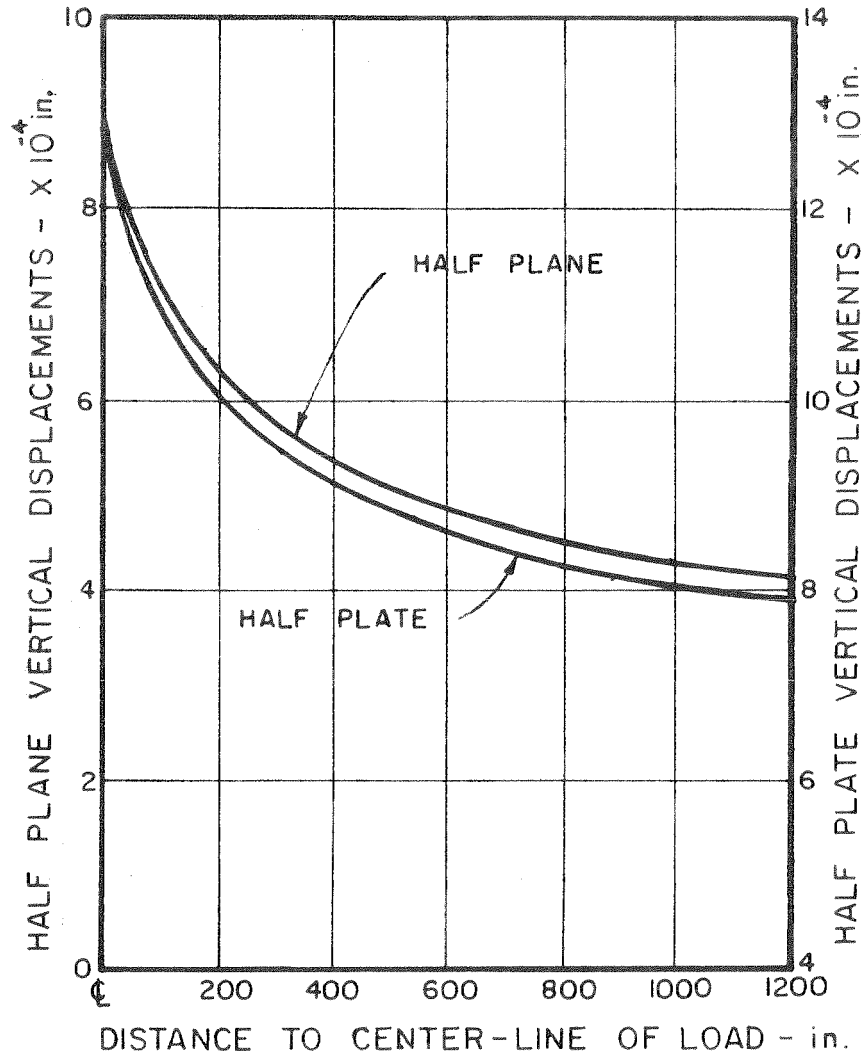FOR INFINITE HALF PLANE

Fig. 14 COMPARISON OF VERTICAL DEFLECTIONS FOR
HALF PLANE UNDER STRIP LOAD AND
HALF PLATE UNDER DISTRIBUTED LOAD
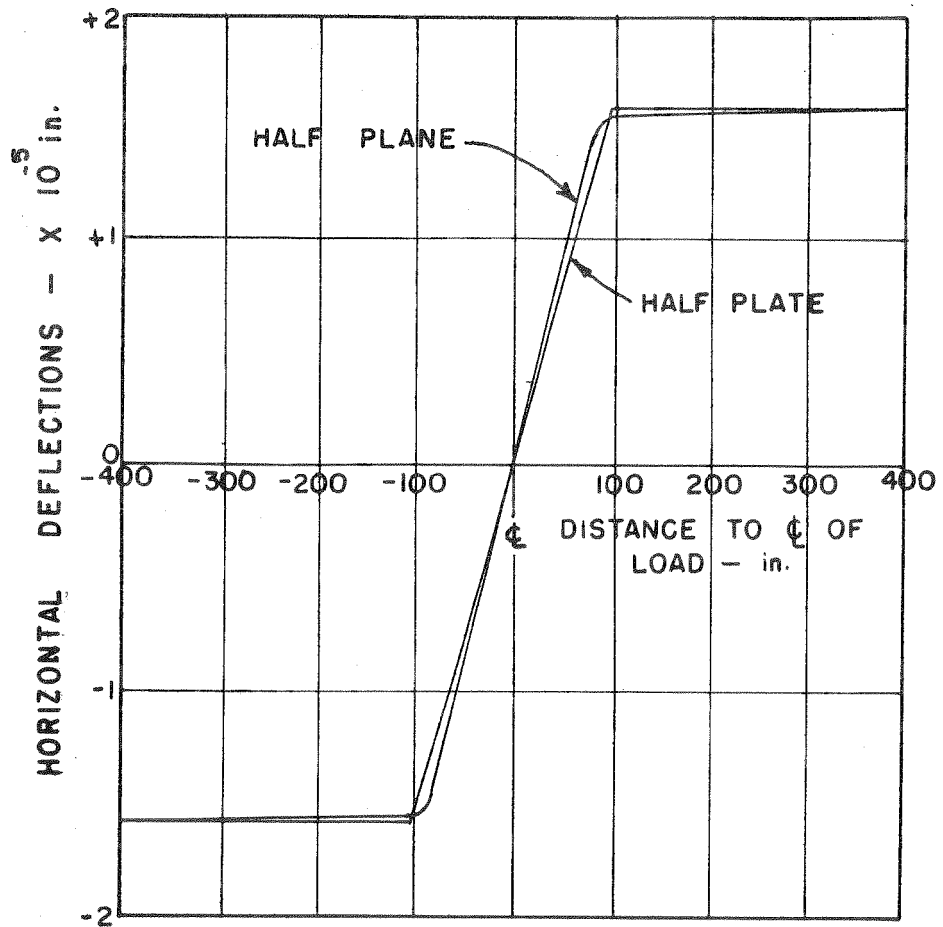
51

Fig. 15   COMPARISON   OF   HORIZONTAL   DEFLECTIONS
FOR   HALF   PLANE   UNDER   STRIP   LOAD   AND
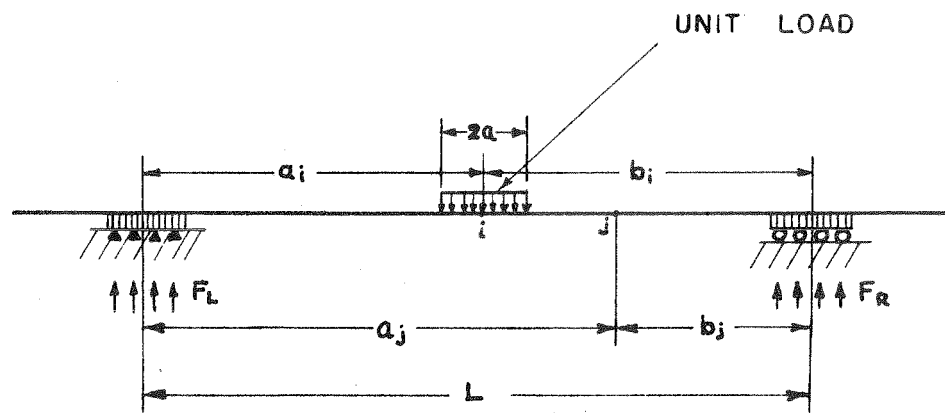HALF   PLATE   UNDER   DISTRIBUTED   LOAD

Fig. 16 SUPPORT CONDITIONS FOR HALF PLATE

considered to be at a long distance from the dam.

The stiffness influence coefficient is defined as the force at an arbitrary point j due to a unit displacement at i. However, because the solution to the problem is formulated in terms of displacement due to load, flexibility influence coefficients will be generated. It is the inverse of the matrix defined by these terms which gives the stiffness coefficients. Because of the support conditions, vertical and horizontal loadings must be treated separately.

Consider a unit vertical load at point i of Fig. 16 and let the point of zero displacement be the left support L, that is $d=a_i$.

There will be three vertical displacements to be summed as follows:

a) vertical displacement due to vertical load at $i = 1$

b) vertical displacement due to vertical load at $L = F_L = -b_i/L$

c) vertical displacement due to vertical load at $R = F_R = -a_i/L$

These are shown in Fig. 17, a, b, c. If u and v represent the appropriate displacements at j due to unit load at i (positive displacement being toward and to the right) then

$$\delta_i = v_{ji}^v - \frac{b_i}{L} v_{jL}^v - \frac{a_i}{L} v_{jR}^v \qquad \text{VI-16}$$

There is, however, a displacement at R, which is not possible under the support conditions. Therefore, a rigid body rotation must be applied to the system to make
$$\delta_R = 0$$

Initially $\qquad \delta_R = v_{Ri}^v - \frac{b_i}{L} v_{RL}^v - \frac{a_i}{L} v_{RR}^v \qquad \text{VI-17}$
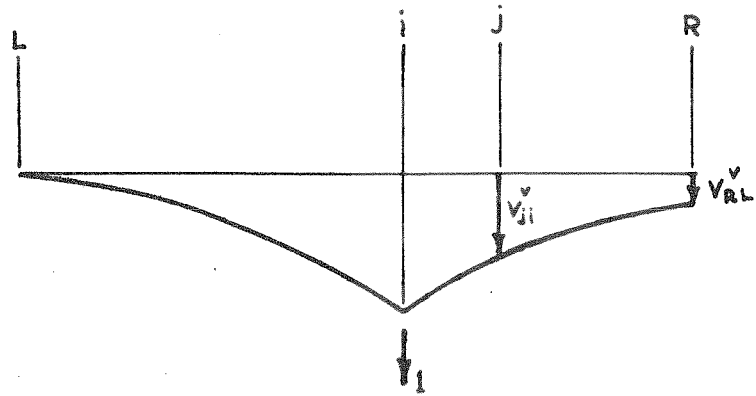
Fig. 17a   LOAD   APPLIED   AT   i
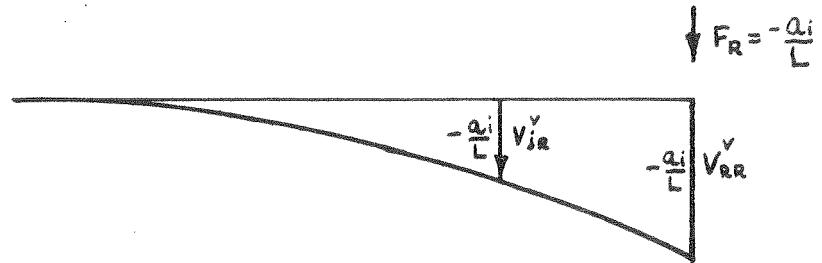

Fig. 17b   LOAD   APPLIED   AT   L

Fig. 17c   LOAD   APPLIED   AT   R

Fig. 17   VERTICAL   DISPLACEMENTS   DUE   TO

VERTICAL   LOADS

The required rotation is, therefore δ_R/L clockwise and

$$\delta_{ji} = v_{ji}^v - \frac{b_i}{L}v_{jL}^v - \frac{a_i}{L}v_{jR}^v - \frac{a_j}{L}\left[v_{Ri}^v - \frac{b_i}{L}v_{RL}^v - \frac{a_i}{L}v_{RR}^v\right] \quad \text{VI-18}$$

All the terms in the above equation may be determined from equation VI-6.

For the horizontal displacements due to vertical load at i, the same sum will apply (see Fig. 18). Again, let $d = a_i$

The horizontal displacement at j is given by

$$\delta_{ji} = u_{ji}^v - \frac{b_i}{L}u_{jL}^v \quad \text{VI-19}$$

In this case, horizontal displacement at R is not restrained, and so no rotation is required.

For the horizontal loads, the sum of only two terms are necessary, the horizontal reaction being entirely at L and being equal and opposite to the applied load. In the case of horizontal displacements, therefore, the sum will be of the two terms shown in Fig. 19 a, b. Again $d = a_i$

with no rotation required

$$\delta_{ji} = u_{ji}^h - u_{jL}^h \quad \text{VI-20}$$

Similarly, for vertical displacements, the terms to be summed are shown in Fig. 20.

Then $\quad \delta_{ji} = v_{ji}^h - v_{jL}^h \quad$ VI-21

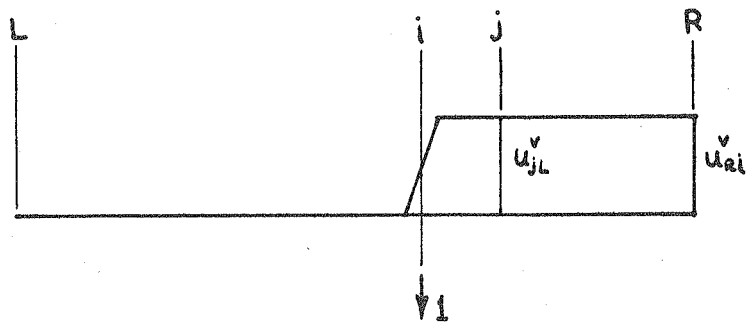and $\quad \delta_R = v_{Ri}^h - v_{RL}^h \quad$ VI-22

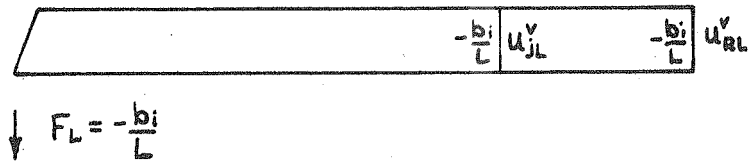Fig. 18a   LOAD   APPLIED   AT   i

Fig. 18b   LOAD   APPLIED   AT   L

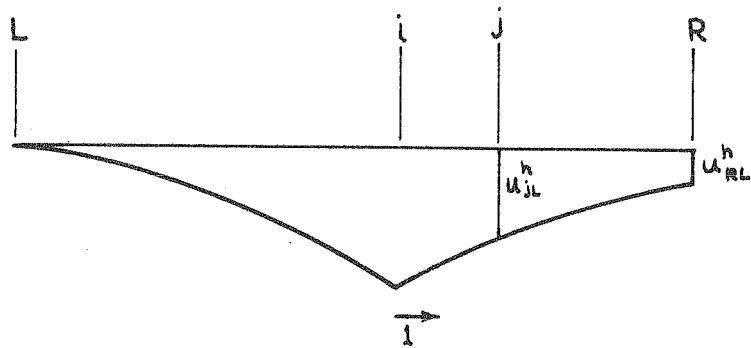Fig. 18   HORIZONTAL   DISPLACEMENTS   DUE   TO
VERTICAL   LOADS
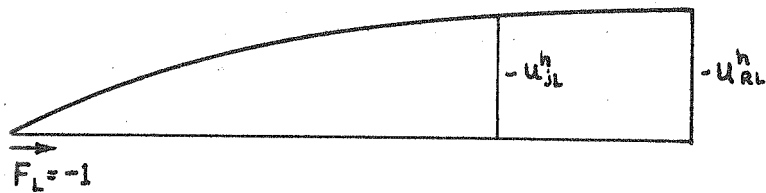
Fig. 19a   LOAD APPLIED AT i

Fig. 19b   LOAD APPLIED AT L

Fig. 19   HORIZONTAL   DISPLACEMENTS   DUE   TO
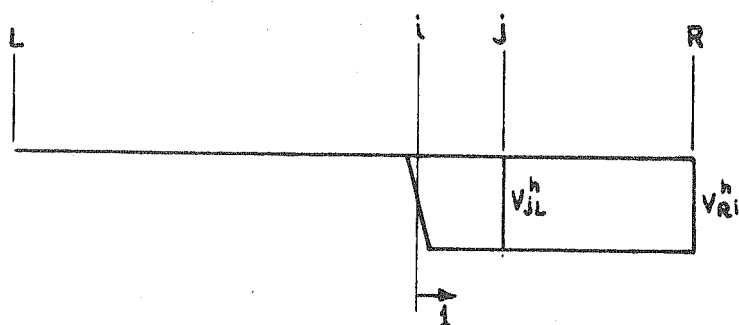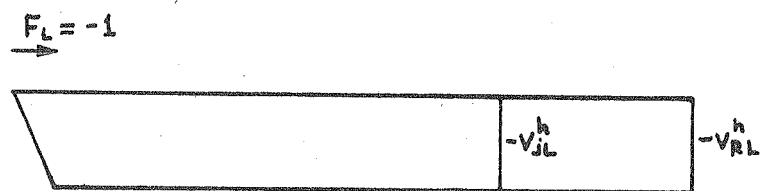HORIZONTAL   LOADS

58

Fig. 20a LOAD APPLIED AT i

Fig. 20b LOAD APPLIED AT L

Fig. 20 VERTICAL DISPLACEMENTS DUE TO
HORIZONTAL LOADS

Thus, a clockwise rotation of δ_{Ri}/L must be applied to make

Then
$$\delta_{ji} = v_{ji}^h - v_{jL}^h - \frac{a_j}{L}\left(v_{RL}^h - v_{RL}^h\right) \qquad\qquad \text{VI-23}$$

The four terms thus given by equations VI-18, 19, 20, 23 may be gathered together to form the flexibility influence coefficient submatrix for the influence of forces at i on a point j.

$$\left[f_{ji}\right] = \begin{bmatrix} u_{ji}^h - u_{jL}^h & \vline & u_{ji}^v - \frac{b_i}{L}u_{jL}^v \\ \hline v_{ji}^h - v_{jL}^h & \vline & v_{ji}^v - \frac{b_i}{L}v_{jL}^v - \frac{a_i}{L}v_{jR}^v \\ -\frac{a_j}{L}\left(v_{Ri}^h - v_{RL}^h\right) & \vline & -\frac{a_j}{L}\left\{v_{Ri}^v - \frac{b_i}{L}v_{RL}^v - \frac{a_i}{L}v_{RR}^v\right\} \end{bmatrix} \qquad \text{VI-24}$$

Notice that when j and i coincide, the two diagonal terms are equal as

$$u^v = v^h$$

in the equations VI-3 through VI-10; and examination of Figs. 17 and 19 show that all the apparently inconsistent terms cancel out. Assemblage of the $\left[f_{ji}\right]$ into a total flexibility matrix $\left[F\right]$ is done simply by substitution of appropriate sub-matrices. The size of the $\left[F\right]$ matrix will be 2n+1 by 2n+1 where n is the number of internal points considered. The extra row and column are created by the effect of a vertical force at R. This row is easily obtained by forming $\left[F\right]$ as a 2n+2 by 2n+2 matrix and then striking out the last row and column.

The final stiffness influence coefficients are then obtained by inverting $\left[F\right]$.

Those stiffness coefficients, when removed as 2 by 2 sub-matrices, are in exactly the same form as the coefficients generated from a triangular element. The terms may be superposed directly into the same stiffness matrix as the element stiffnesses to form the total stiffness matrix of the structure. The support conditions consist only of a pin at joint L and a roller at R. The point L may be ignored in solution and R is treated as a point with horizontal freedom only.

Fig. 21 shows the results of an example where the structure above the half plane was made very weak compared to the half plane. The solution predicted by the exact theory is also included, and comparison shows that the agreement is quite good.

The measure of accuracy of the solution is dependent upon how well compatibility is maintained across the interface. Since in most dam problems the loading is not concentrated, the displaced lines of the dam and those of the foundations will not be sharply curved, and the solution will be acceptable.
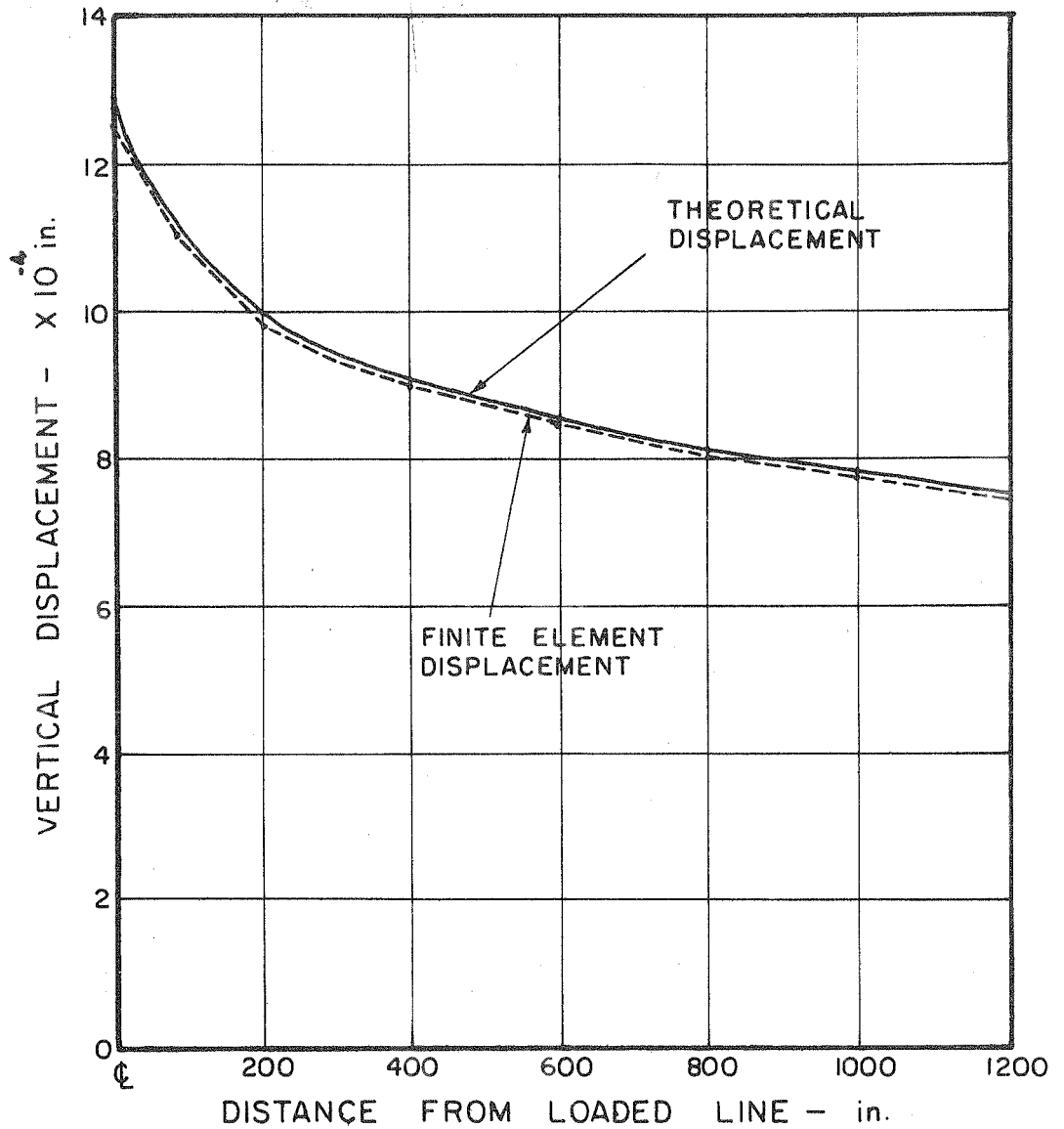
Fig. 21 COMPARISON OF THEORETICAL AND COMPUTED
VERTICAL DISPLACEMENT OF HALF SPACE

VII

COMPUTER PROGRAM

It is necessary to use a high speed digital computer to analyze
time-dependent two-dimensional stress systems by the finite element
method. For a practical analysis, the number of simultaneous equa-
tions soon becomes measured in hundreds rather than tens. The computer
program written to solve this problem consists in its original form of
the program used by Wilson.[6] However, the methods used by Wilson have
had to be entirely revised so as to increase program capacity without
too much increase in unit computing time; or, in parallel, to make
possible storage of the many time-dependent functions involved with-
out decreasing capacity.

When it is necessary to analyze systems with large areas to be
covered, but only small areas where the stresses are of interest, the
need for greater capacity becomes apparent. In this case, it is
necessary to cover the whole outer area with progressively larger
elements, and the location of interest with a fine mesh of small
elements. The net result is a large number of elements with an
irregular layout. The computation of the necessary data arrays for
the input data then becomes a significant problem.

An early approach to the solution of this problem[17] was to use
two passes in the analysis. In the first pass, the system was
analyzed with a coarse mesh covering the whole area. The resulting
displacements at a "reasonable distance" from the point of interest

were then used as displacement boundary conditions in the second pass.

The second pass used a fine mesh over the entire area, the loading was

the original applied external forces for that part of the system. Linear

interpolation was used to obtain displacements for new points which lay

between the original nodal points. The procedure is illustrated in Fig.

22 where a section near a crack was removed and a fine mesh substituted

in this area.

The method has an inherent weakness because the resulting stresses

are only as good as the displacements on the boundary, and it is hard

to define a "reasonable distance" for the effect of the mesh size to

be minimized.

The two-pass approach breaks down completely when areas exist with

different material properties and the coarse mesh then must be made to

cover these areas with a sufficiently good representation of this effect.

A program with very large capacity has an important simplifying

advantage of making uniform meshes possible with the fineness spreading

over a greater area. It is also necessary to make only one pass on the

computer and make no intermediate changes. The time that is lost by

the increased size of the single analysis is easily made up by these

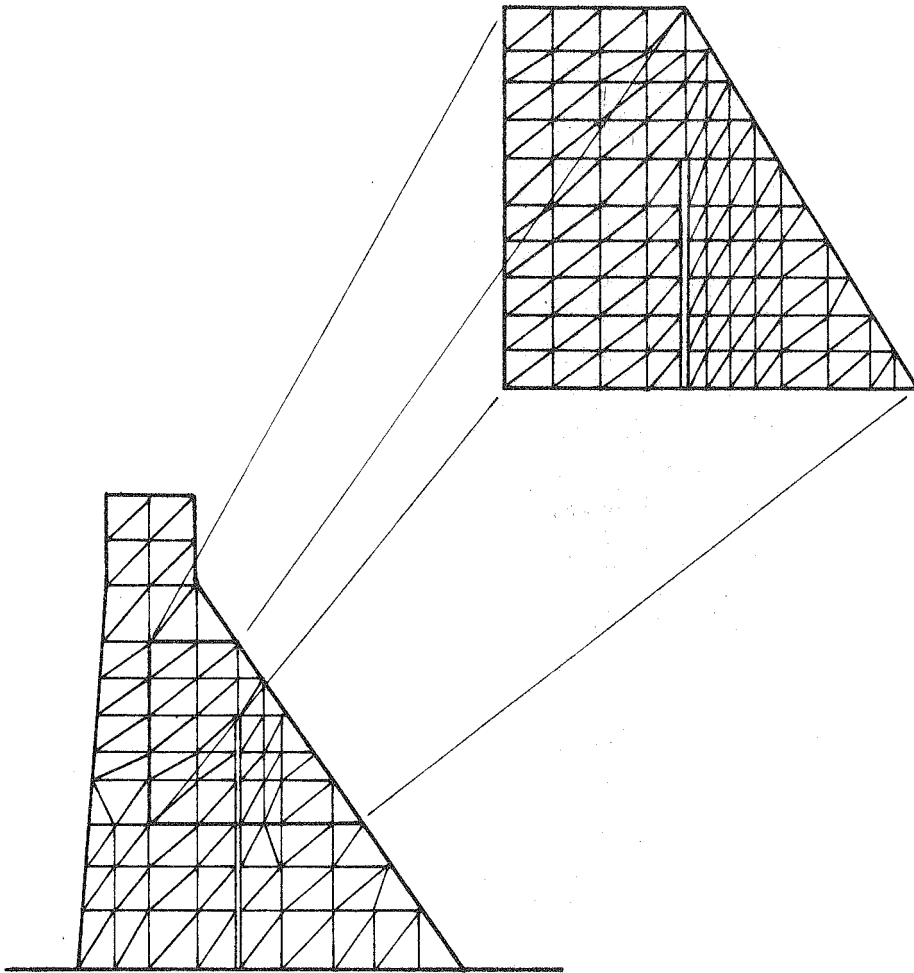simplifications.

Fig. 22   REMOVAL   OF AREA   OF   FINE   MESH
FROM   COARSE   MESH

THE ITERATION PROCEDURE

The basic solution by iteration of the Gauss-Seidel type depends

upon repeated application of the equation.

$$V_n^{s+1} = k_{nn}^{-1} \left\{ R_n - \sum_{i=1 \neq n}^{N} k_{ni} v_i^s \right\} \qquad n = 1, N \qquad \text{VII-1}$$

where V_n and R_n are two element vectors of displacements and forces

respectively, using rectangular cartesian coordinates, at the nodal

point i. k_{ni} are the two by two stiffness influence coefficient

matrices of the whole structural stiffness matrix taken one nodal

point at a time. s is the superscript indicating the number of itera-

tions applied. This method may be improved by splitting the summation

term and using the values v_i^{s+1} for i = 1, n-1 which have already been

calculated in this cycle. This is the accelerated Gauss-Seidel

iteration procedure. The equation for iteration on the point is then

$$V_n^{s+1} = k_{nn}^{-1} \left\{ R_n - \sum_{i=1}^{n-1} k_{ni} v_i^{s+1} - \sum_{i=n+1}^{N} k_{ni} v_i^s \right\} \qquad n = 1, N \qquad \text{VII-2}$$

This method uses all terms in the total stiffness matrix, it is

possible to skip all the zero elements by simply labelling the terms

that are non-zero. Solution may also be speeded by the use of over-

relaxation where the computed change in displacement for any one cycle

is multiplied by a factor between one and two. The above procedures

were incorporated by Wilson[6] into his program.

The modification described below is dependent on the symmetry of

the stiffness matrix. The terms k_{ni} for $i < n$ represent the submatrices

which are below the leading diagonal of the array.

Since

$$k_{ni}^{T} = k_{in}$$

<div align="right">VII-3</div>

the influence coefficients for the upper triangular part are all that are

required. The computer storage for the non-zero terms is approximately

halved, all that is needed is a reference table to give the symmetrical

elements. Physically, the terms $k_{ni} v_{i}'$ of the summation represent the

unbalanced forces at a point n due to a displacement v_{i} at i. A conven-

ient way to simplify calculation is to compute the values of the unbal-

anced forces, due to displacements at i, at the connected points which

have nodal point numbers greater than i. These points represent the

terms which appear on the upper off diagonal part of the rows connected

with i. This means that when the point n is reached in the iteration

cycle, the term $\sum_{i=1}^{n-1} k_{ni} v_{i}^{s+1}$ will have already been computed and no summation

will be required for the lower diagonal terms. Equation VII-2 may then

be given the form

$$v_{n}^{s+1} = k_{nn}^{-1} \left\{ R_{n}^{u} - \sum_{i=n+1}^{N} k_{ni} v_{i}^{s} \right\}$$

<div align="right">VII-4</div>

where

$$R_{n}^{u} = R_{n} - \sum_{i=1}^{n-1} k_{in}^{T} v_{i}^{s+1}$$

<div align="right">VII-5</div>

To compact storage further, it is convenient to compact this form

of stiffness matrix by omitting all zero terms in the symmetrical part.

These changes have enabled the capacity of the computer program to be

increased from 350 to 600 points. The speed of operation is virtually

unchanged, the rate of convergence is identical.

The computer program was then modified to include the effects of

time-dependent properties. The changes consisted of inserting a

section to calculate the stress relaxation and the resulting pseudo-

loads, and causing the program to recycle in elastic solution.

The flow chart shown below is intended to indicate only the main

outline of the operations; for simplicity, detail has been deliberately

omitted.
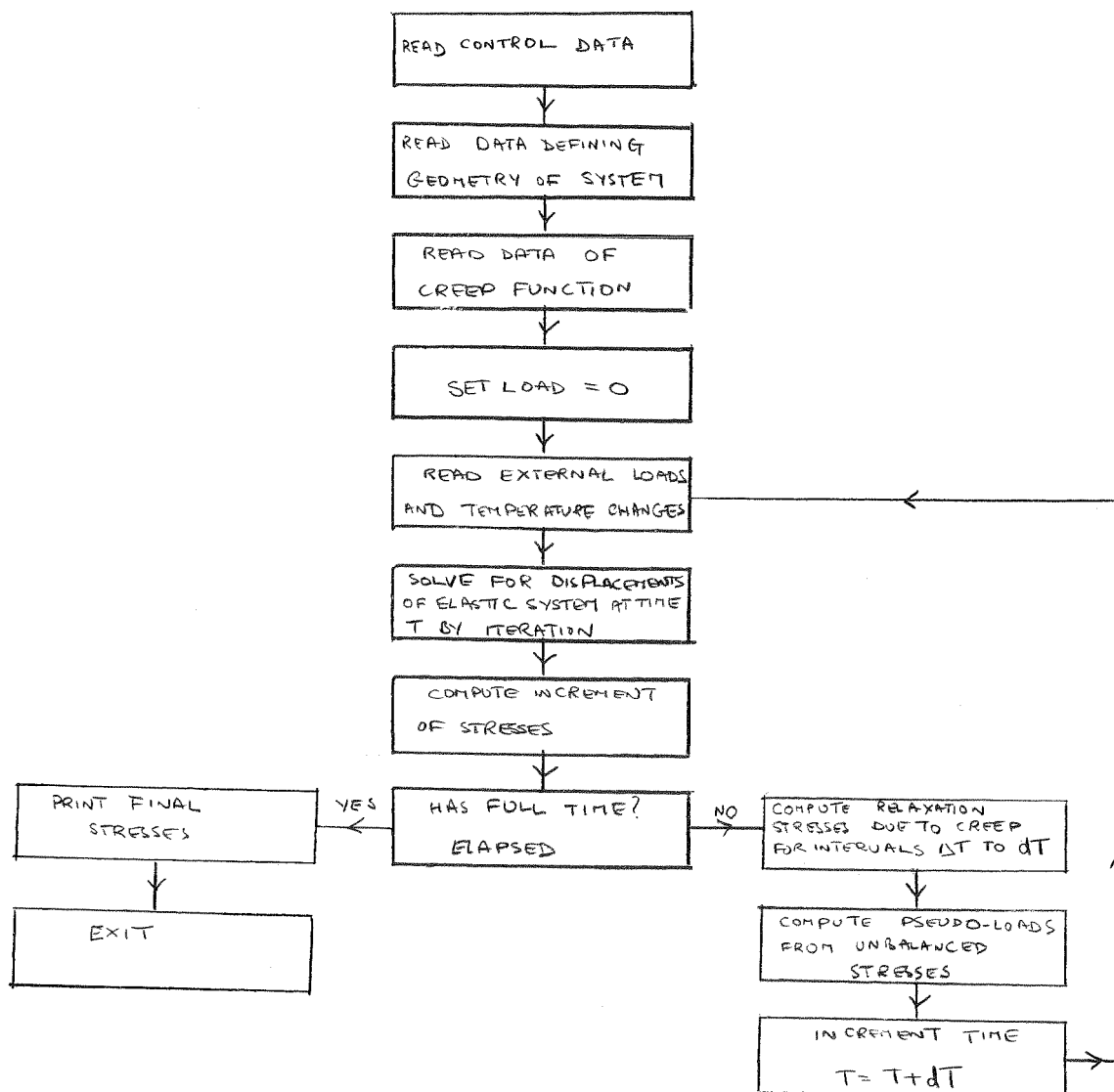
VIII

THE APPLICATION OF AUTOMATIC PLOTTING PROCEDURES

With the increase in the number of nodal points made available by the program, there arises a purely mechanical problem in the generation of triangular meshes, the checking of the meshes and the interpretation of the results. The automatic plotter may be used to simplify some of these tasks. It is both laborious and difficult to create and punch a satisfactory system correctly at the first pass. Some concept of an automatic generator which defines the elements is required then the plotter may be used to check the resulting mesh.

The generation of a random mesh which can be optimized to make each triangle as nearly equilateral as possible is a complicated but not impractical procedure. A simpler approach will, however, be described. This recognizes that in most structures it is possible to introduce a series of parallel lines slicing the structure, and these lines need not be a constant distance apart. More lines may surround any area of particular interest. Strictly the lines need not be parallel, but the generation of meshes is much simplified if they are.

Examination of the single layer shown in Fig. 23a indicates that a regular numbering sequence may be used to define the elements

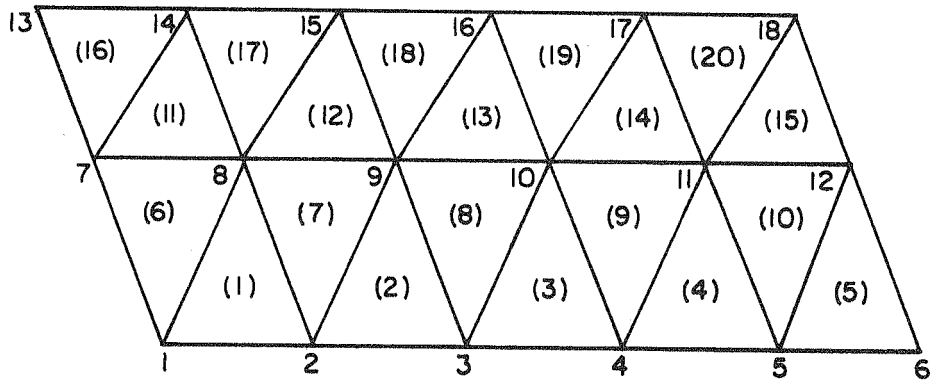| i.e.,	element	i point	j point	k point
	1	1	2	7
	2	2	3	8
	3	3	4	9
	---	---	---	---
	6	7	2	8
	7	8	3	9
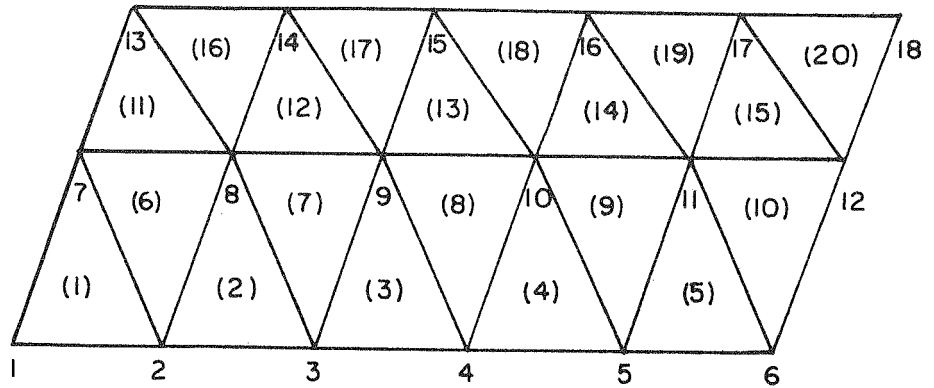
(a) ALTERNATE 1

(b) ALTERNATE 2

Fig. 23 TYPICAL TRIANGULAR ELEMENT LAYOUTS

All that is required of a generating program is that it set up the correct coordinates for the nodal points and then construct the element array to coincide with the form shown above. A restriction of this method, is that the number of nodal points in a row may only change by one between adjacent rows. Sharply changing sides of a system will not be easily or well generated. A further problem arises from the need to select between two possible forms of arrangement represented either by connecting 1 2 7 or 1 2 8 in the mesh as shown in Fig. 23 a, b. In this case, there must be some decision made which gives the better set of triangles. This leads to deciding upon which outer sides have the greater slope and using this to decide the starting triangle.

An automatic mesh generating program has been written which takes as input the coordinates defining the boundary and the number of points that are wanted on any one line. Weighting factors may be read in which cause the nodal point spacing on a line to be non-equal and allow fine meshes to be created in a specific area. The program generates and punches all the coordinate points of the mesh as well as the element arrays which locate the triangles. The final part of the program draws the mesh that has been generated on an automatic plotter. This makes possible swift checking of the arrays to make sure the problem is satisfactorily defined. Fig. 24 shows a typical output plot. Note that the parallel lines may be skewed in any direction by a simple rotation transformation.
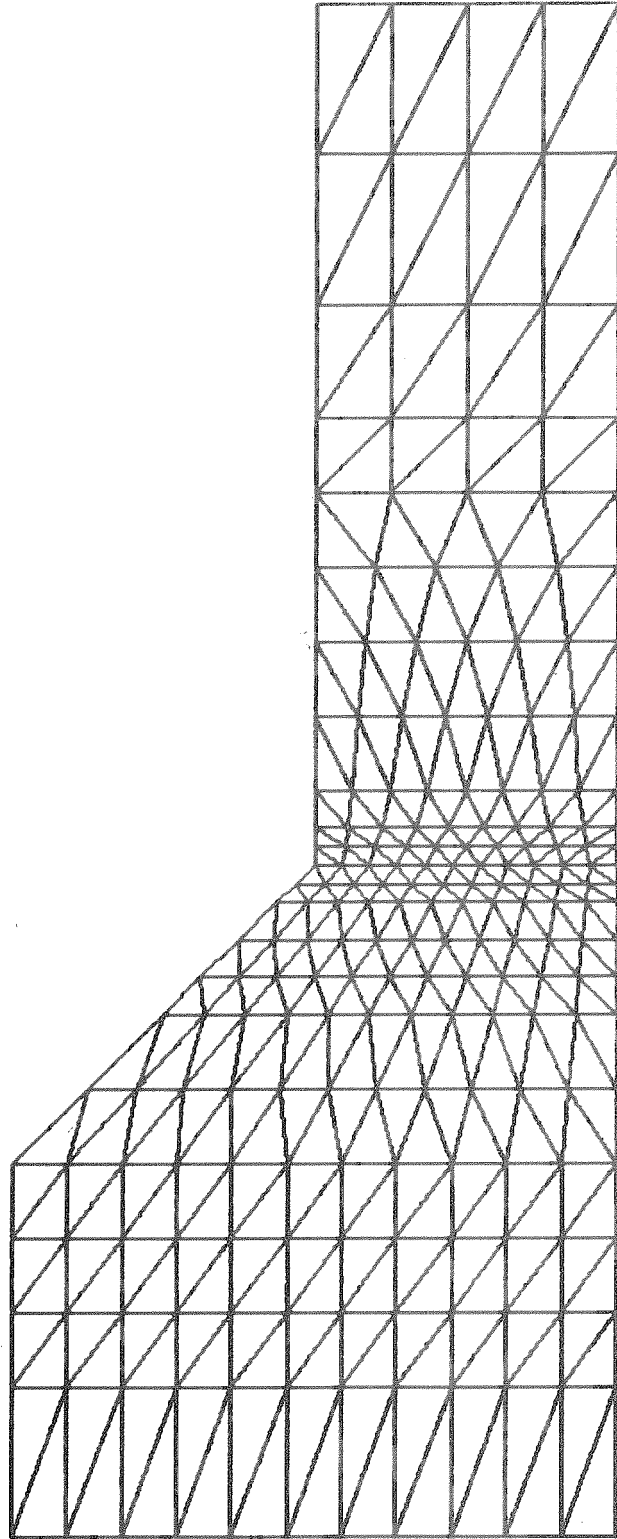
Fig. 24   TYPICAL MESH   GENERATED   BY
AUTOMATIC   PLOTTER

INTERPRETATION OF RESULTS

The interpretation of results from the finite element program is a problem of much repetive work. It involves transferring output information onto some form of plot, either isotatic lines (otherwise called stress contours), stress vectors, stress trajectories, or stresses across a section. The automatic plotting machines which may be run from magnetic tape through subsiduary equipment to the main computer, make possible the automatic interpretation of the results. A scheme will be discussed which takes the output stresses of the program and then generates the line of action of the isostatics. These isostatics are superimposed upon an outline of the system. The formulation of stress trajectories is then described.

Let σ_{x_1}, σ_{x_2}, σ_{x_3} represent the values of a stress component at the nodal points of an element. These values may be obtained from element stresses by extrapolation or interpolation procedures, such a procedure was proposed by Wilson.[6] The distribution of these stresses over the element will be assumed to be in the form of a plane passing through the three values at the vertices. Comparison of the values at the vertices enables an order to be established, for example. $\sigma_{x_2} < \sigma_{x_1} < \sigma_{x_3}$ Then if a prescribed contour value lies between the largest and smallest values, a contour of this value exists on the element. Linear interpolation along the sides may now be used to get locations for the ends of the contour in this element. A straight line constructed between these ends then forms the contour of this element.

The procedure may be repeated for different values of contours until they fall out of the range of the stresses over the element. It should be noted that stress contours over any element will be parallel. Then, if the whole scheme is repeated for each element, a complete picture of the isostatics for the entire structure will be formed. The contours will match at the element boundaries but will not have the same slope. The degree of smoothness of the curves produced will depend on the fineness of the mesh used. An example of such a plot is shown in Fig. 25. Any component of stress may be plotted in this way.

Of frequent interest to the practicing engineer are the trajectories of principal stress or shear. These are not lines of constant value, but lines that have the same directions as the principal components at any point.

The values of stress at any interior point of a triangle lie on the plane formed by the values at the vertices, therefore, these values may be simply obtained from matrix algebra. Let the triangle under consideration have coordinates at the vertices i, j, k of $(0,0)$, (x_j, y_j), (x_k, y_k) and coordinate stress values f_i, f_j, f_k (for σ_x stresses for example). Then the value at (x,y) is given by

$$f = ax + by + c \qquad \text{VIII-1}$$

where a, b, c are constants. From the known values, a matrix equation may be written

$$
\begin{bmatrix}
0 & 0 & 1 \\
x_j & y_j & 1 \\
x_k & y_k & 1
\end{bmatrix}
\begin{bmatrix}
a \\
b \\
c
\end{bmatrix}
=
\begin{bmatrix}
f_i \\
f_j \\
f_k
\end{bmatrix}
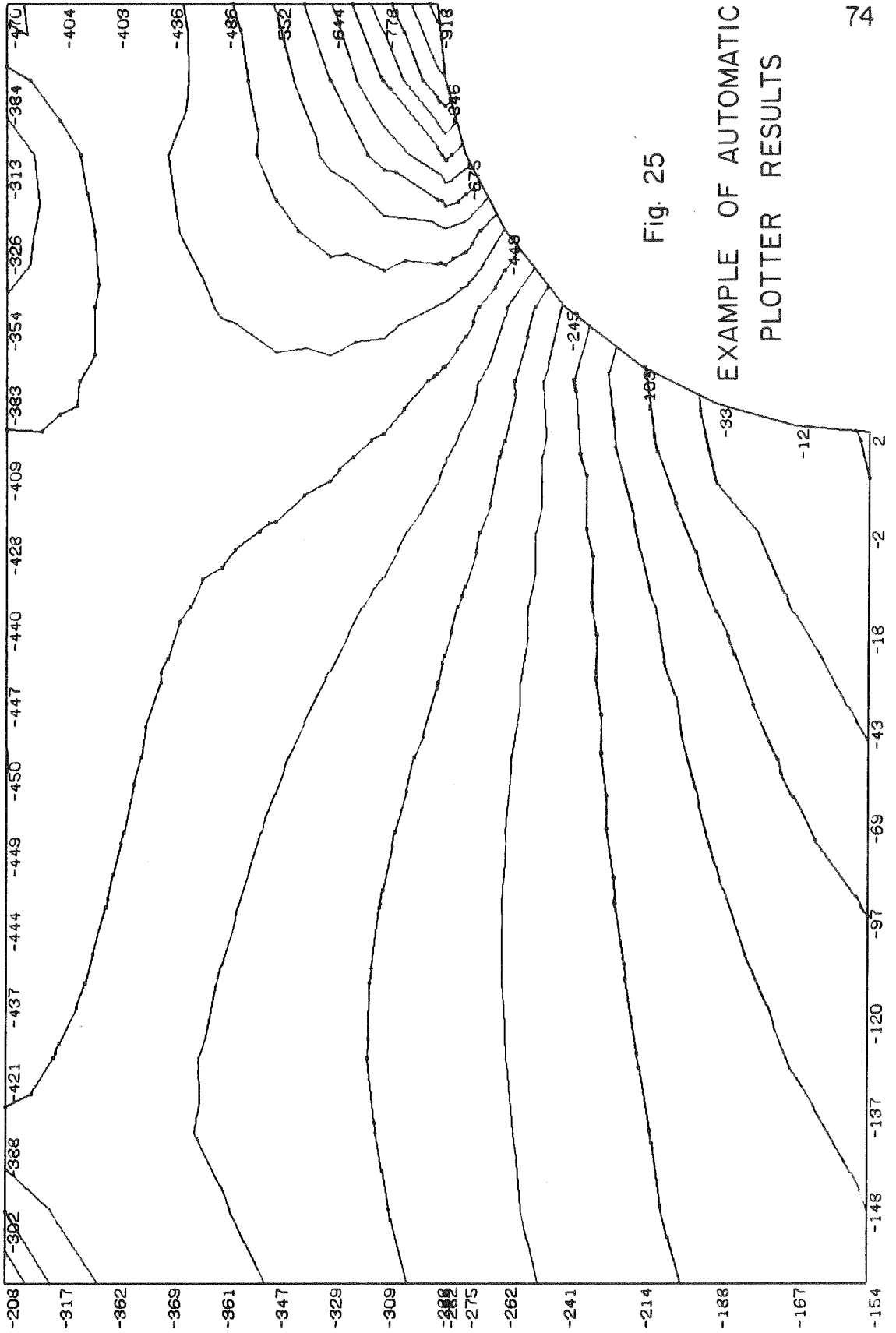\qquad \text{VIII-2}
$$

SIGMA XX

Fig. 25

EXAMPLE OF AUTOMATIC
PLOTTER RESULTS

Solving this equation

$$a = \frac{(f_j - f_i)y_k - (f_k - f_i)y_j}{x_j y_k - x_k y_j}$$ VIII-3

$$b = \frac{(f_k - f_i)x_j - (f_j - f_i)x_k}{x_j y_k - x_k y_j}$$ VIII-4

$$c = f_i$$ VIII-5

Thus the values for σ_x, σ_y, σ_{xy} may be obtained for any interior point (x,y). From these values, the direction of the component of interest may be computed. For example, the direction of the maximum stress is given by

$$\theta = \frac{1}{2} \tan^{-1}\left(\frac{2\sigma_{xy}}{\sigma_y - \sigma_x}\right)$$ VIII-6

A given stress trajectory may thus be followed in its path across a triangle by taking a given starting point and constructing a line of some specified length with an angle appropriate to the mid-point of the line. The length may be made sufficiently short that when the new point is used as a starting point a true curve is approached. The procedure is repeated from point to point until an element boundary is crossed, at this time a new plane is used for the component stresses and the process repeated across this element. The complete process is repeated until the boundary of the structure is reached. To create a complete set of trajectories, the method may be repeated for a variety of starting points, these may be interior points or boundary points.

A simpler method than this is to take the element stresses and use these to define a straight line to cross the whole element. With a sufficiently fine mesh, this works very well, as may be seen in Fig. 26 which represents the lines of maximum shear in an embankment that has been cut down into a rock material.

The construction of section plots is a trivial extension of the contour plotting routine and needs no further description.
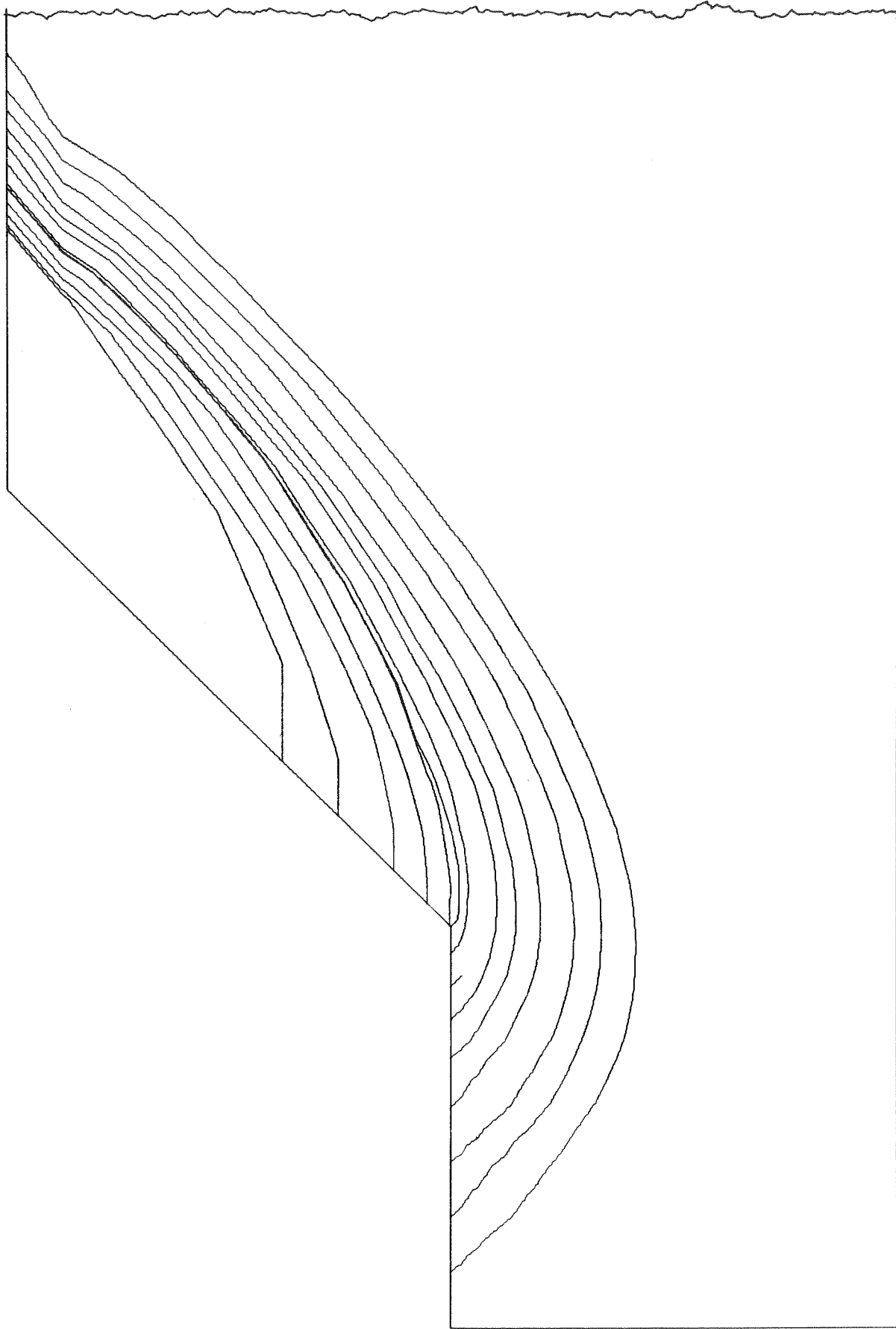
Fig. 26   TRAJECTORIES OF MAXIMUM SHEAR – EXAMPLE PLOT

IX

EXAMPLES

Two examples will be analyzed and the resulting stress distributions discussed.

Example I, a gravity dam, was selected as an example of practical analysis of a real structure where the answers obtained have a real significance in the design of cooling procedures for concrete. It is also important in deciding the frequency or need for longitudinal joints.

Example II is a demonstration of the variation of stress that can occur with creep. It also shows the use of automatic plotting programs in the direct interpretation of results.

EXAMPLE I: THE ANALYSIS OF A STRAIGHT GRAVITY DAM

A gravity dam is built of a series of lifts of concrete placed at fairly regular intervals. The dam is, therefore, made of a series of discontinuous layers. The purely elastic analysis of such a dam does not give a true indication of the state of stress. It is not entirely satisfactory to assume that the stresses due to dead weight suddenly appear in the completed structure. The stresses, in fact, build up while the dam is under construction. Of more significance, however, is the fact that the thermal stresses caused by the alternate heating and cooling of the hydrating concrete cycle also act as the dam is built. Much of the change of temperature occurs at an early age in each indivi-dual lift, and at this time there will not be much material above the area in question that can resist deformation. The thermal stresses are

dissipated by creep so that after long enough time they can be expected to be much reduced.

A more realistic distribution of stress is thus given by an analysis which takes into account the changing geometrical configuration during construction and also the creep of the material. The change in geometry is easily accommodated in the analytical procedure because the step by step solution of the visco-elastic problem of creep requires a series of time steps between analyses. All that is required is to install an additional group of elements at the instant before analysis and use the dead load of the added material as additional external loads in the finite element analysis. Because the layer on the surface is poured in fluid form, it causes no shear forces in the old surface. This condition is approximately by giving the new material a very low modulus of elasticity at the time of placement.

The example will analyze the first 18 layers of a straight gravity dam of the dimensions shown in Fig. 27. The construction sequence is defined in Fig. 28.

The dimensions of this problem lead to the need for many elements in a layer if it is designed to keep the triangles approximately equi-lateral. The ratio of height to length for a single layer is 1 to 134 and at least 100 elements would be needed for a single layer. However, the expected nature of the results show that the stresses in the middle of the section should be uniform with respect to horizontal position.
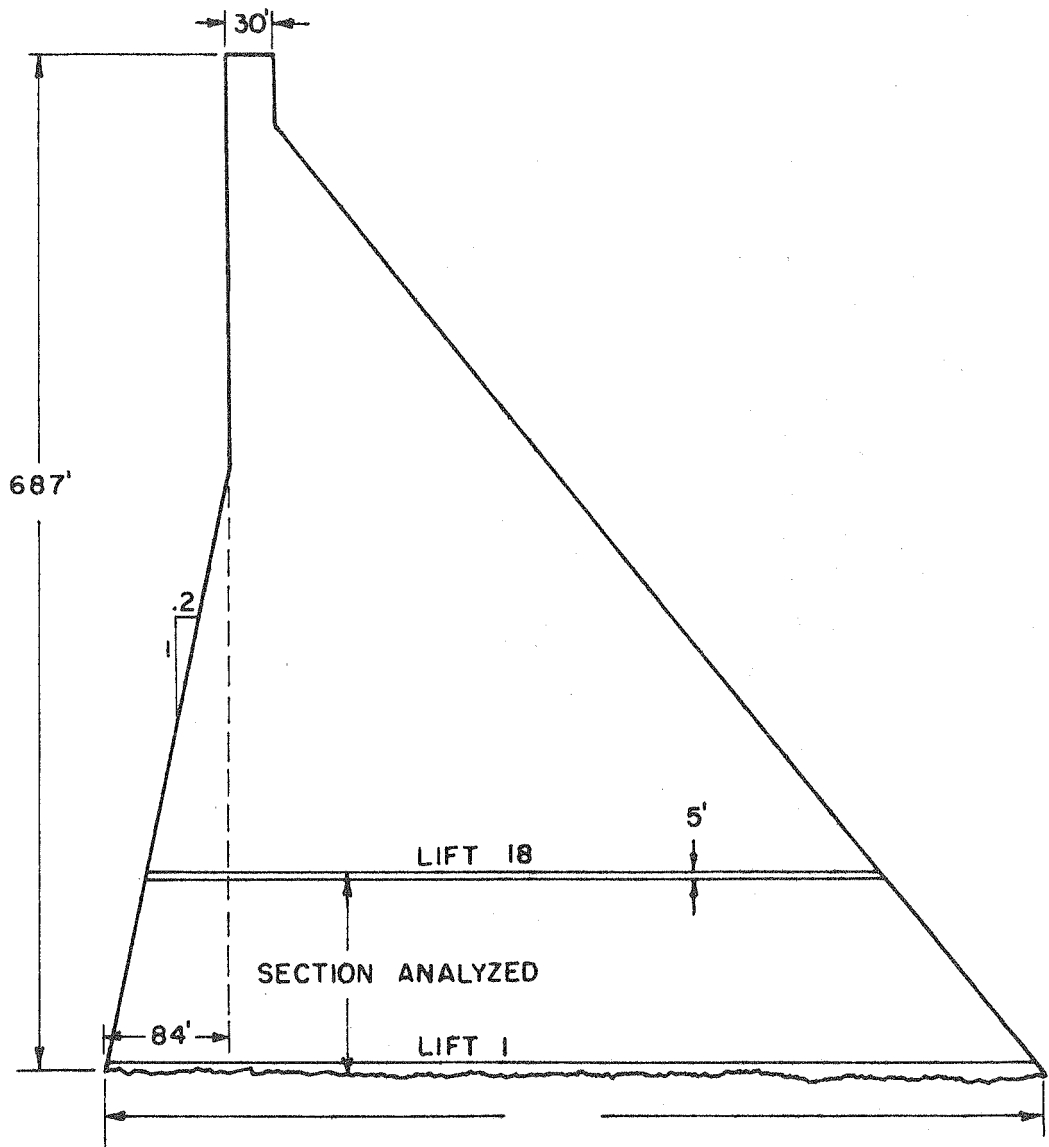
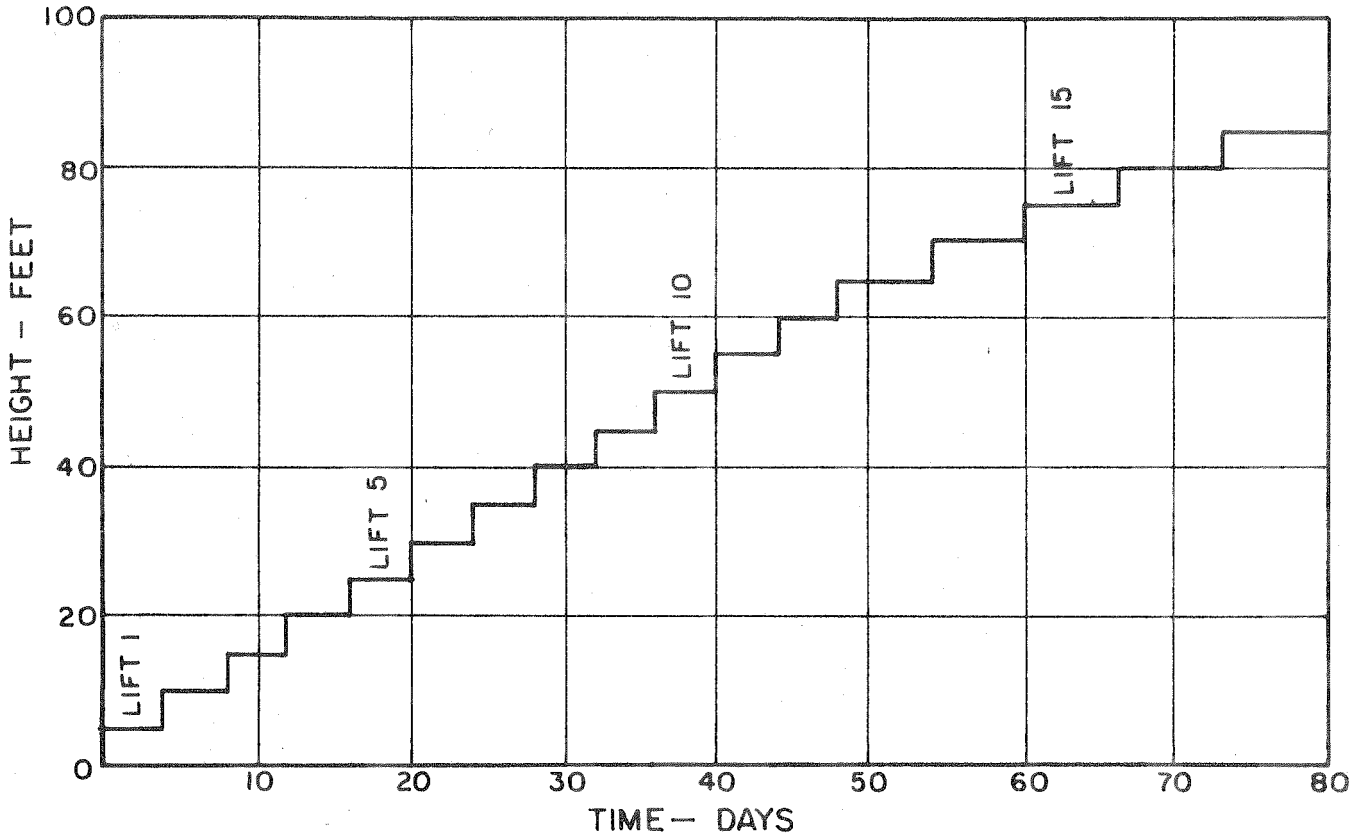Fig. 27   TYPICAL   CROSS   SECTION   OF   EXAMPLE   1

Fig. 28   ASSUMED   CONSTRUCTION   SEQUENCE

Therefore, it is possible to select elements that are very long and flat, and reduce the number of elements to about 20. The results of a comparison analysis are shown in Fig. 29 and the close agreement at the center between results obtained with equilateral and with elongated elements is apparent.

The procedure demonstrates a generally applicable approach to the problem of systems with large areas. It is feasible to take elements that are elongated in shape and get acceptable answers if the stresses in the real system over the area of each element are approximately constant. The triangular mesh system used in a typical layer finally used is shown in Fig. 30.

To investigate the length of time interval required between complete analyses of the system, preliminary analyses were carried out with different time intervals. The results are shown on Fig. 31, they indicate that a 2-1/2 day interval has no significantly different result from a 1-1/4 day interval. The interval required for numerically integrating the relaxation function to generate the pseudo-loads is discussed in the second example.

For purposes of this analysis, temperatures of each lift were assumed to be constant over the whole area at any one time. The temperature variations with time of typical lifts are shown in Fig. 32.

The concrete of the dam was assumed to have the creep properties described in Chapter IV. The variation of instantaneous modulus of elasticity was assumed to be

$$E = (1.0 + 0.667 \log_e t) \times 10^6 \text{ psi}$$

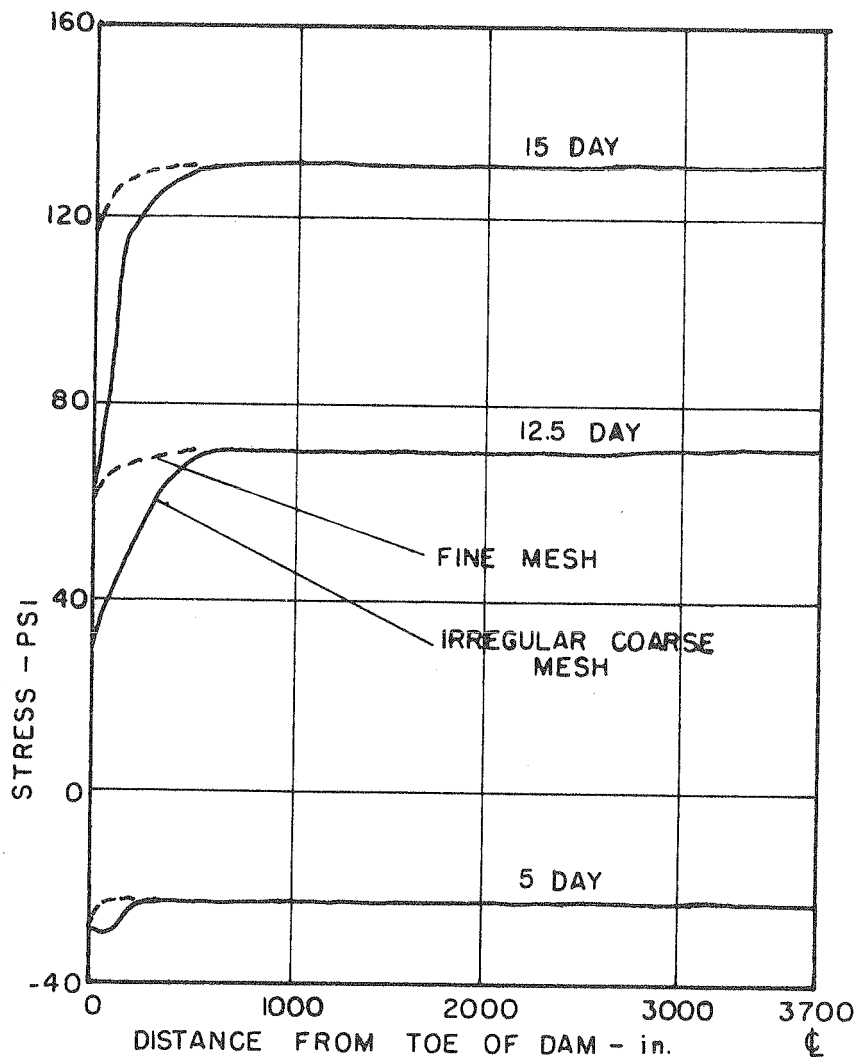The Poisson ratio was assumed to be a constant at 0.17.

Fig. 29   EFFECT OF IRREGULAR COARSE MESH
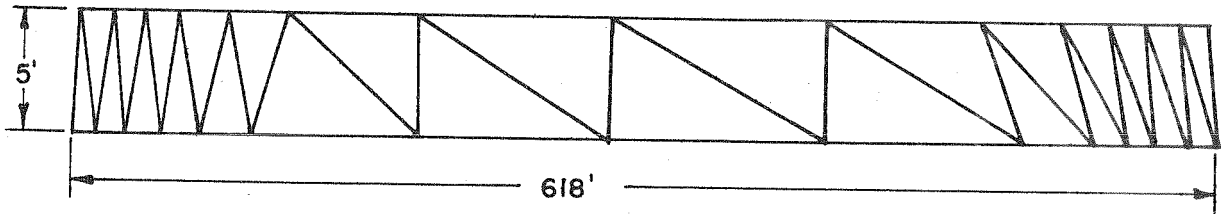
84

Fig. 30   MESH   LAYOUT   FOR   TYPICAL   LAYER
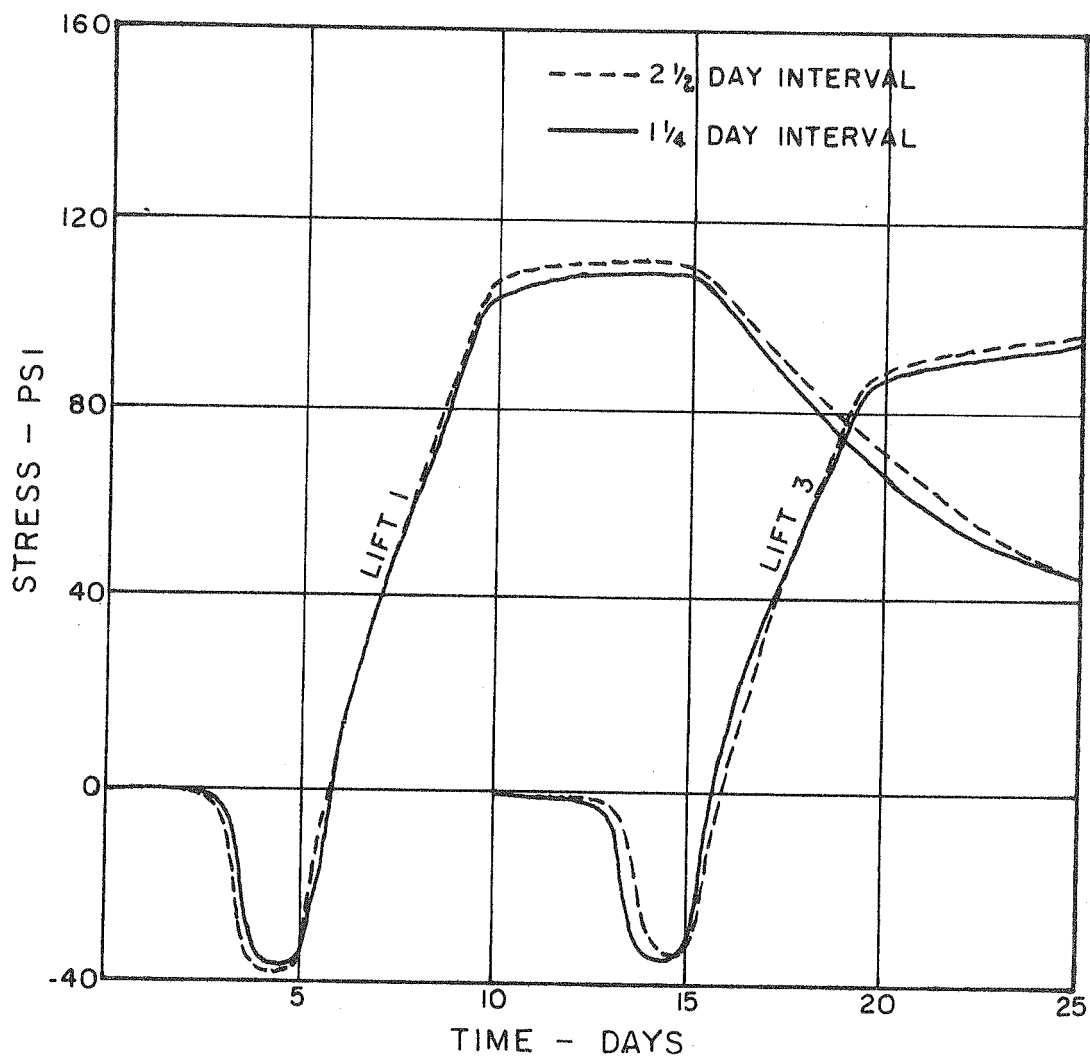
(DISTORTED   SCALE)

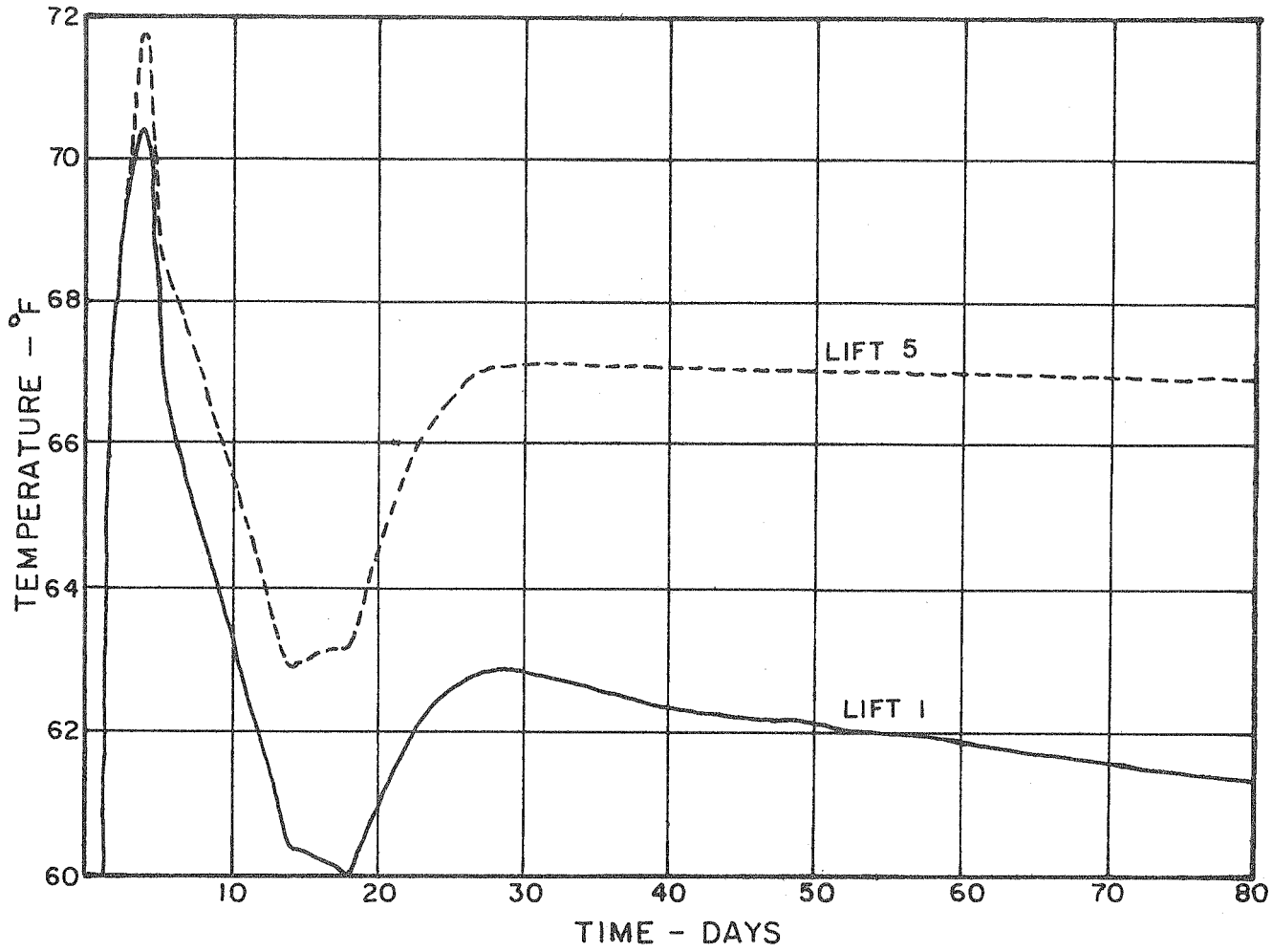Fig. 31 EFFECT OF INTERVAL BETWEEN COMPLETE
SOLUTIONS

Fig. 32   TYPICAL   TEMPERATURE   VARIATION
APPLIED   TO   EXAMPLE   I

Figs. 33 and 34 show the stress distributions resulting from this analysis. Fig. 33 is a plot of mid-section horizontal stress against time for selected layers. Comparison with the temperature history shows the expected rise in stress as the temperature falls. The effect of creep is apparent in the tapering off of the rise despite the still falling temperature. Similarly, the layers above and below have an effect, either increasing or decreasing the stress as is apparent from the figure. Fig. 34 shows the variation with position of horizontal and vertical stresses in the first lift. The time is assumed to be 14 days after the first lift was placed. The figure indicates quite clearly that the edge effects are quite local and most of the layer is under a constant stress. The vertical stresses at this time are essentially uniform and represent only the dead load stresses.

From this analysis, it is clear that with the cooling cycle applied, the stresses reached in the concrete are tolerable. There is no need for longitudinal construction joints. If such joints were used, they would need to be less than 50 ft. apart since that is the limit of the end effects.
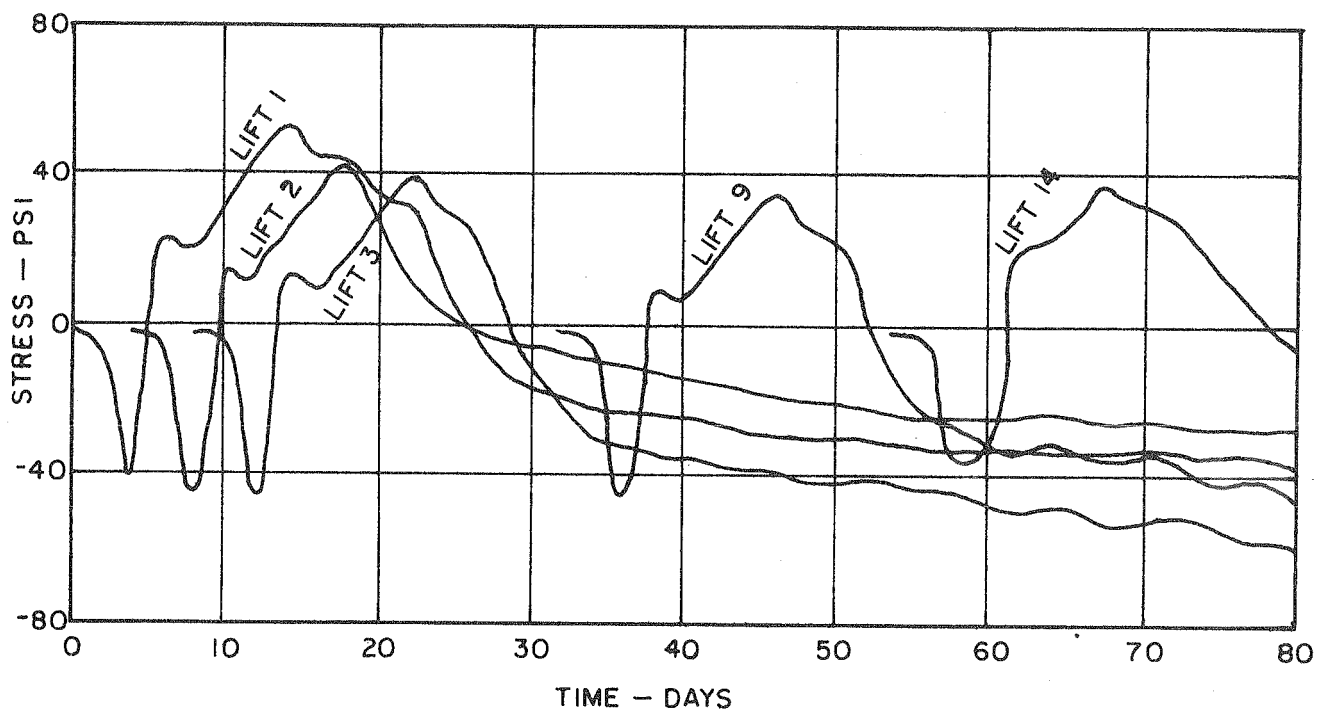
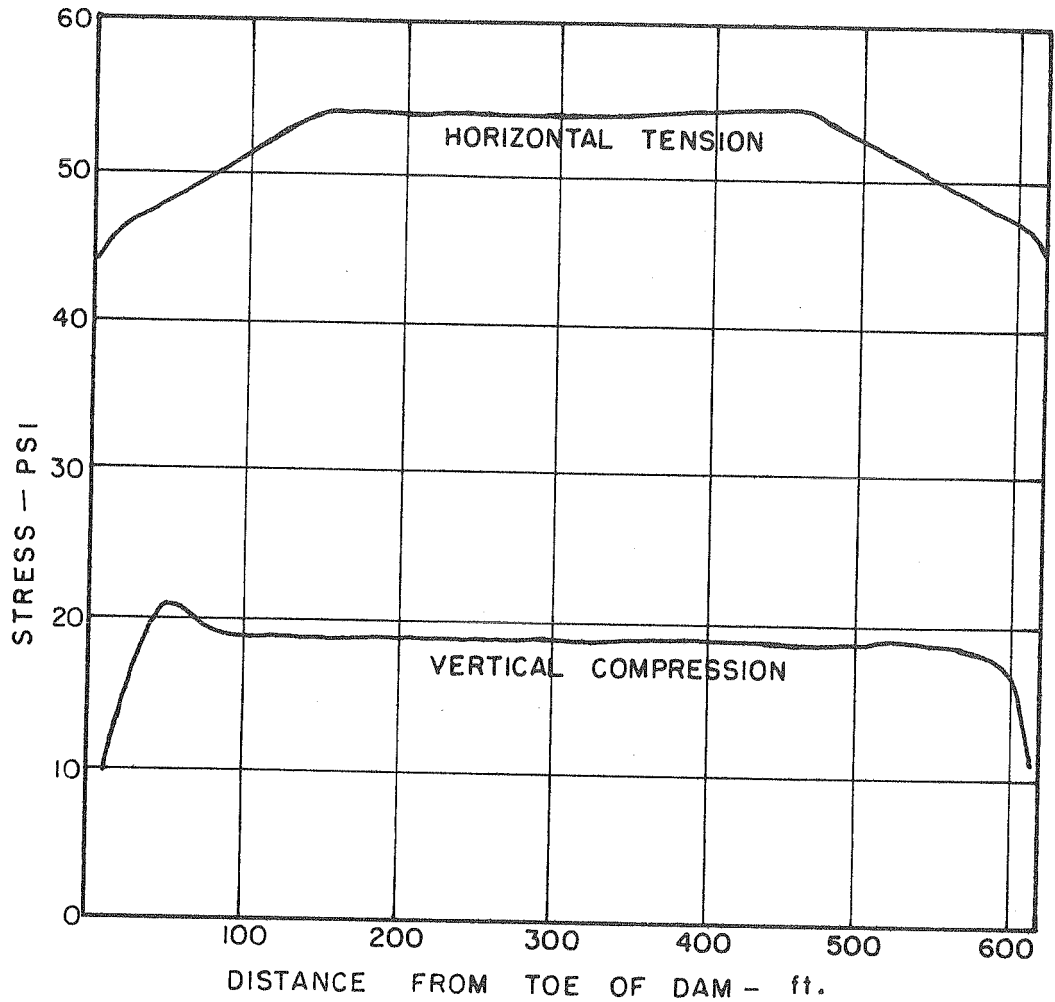Fig. 33   MID-SECTION   HORIZONTAL   STRESS-HISTORIES vs. TIME

Fig. 34   DISTRIBUTION   OF VERTICAL AND HORIZONTAL
STRESSES   IN   LIFT 1 AT 14 DAYS

EXAMPLE II - THE ANALYSIS OF A THIN PLATE INCLUDING

THE EFFECT OF CREEP

The second example has been constructed to show the redistribution of stresses that can occur in a given system when creep in concrete is considered. The geometry of the system and the triangular element layout are shown in Fig. 35. The problem is to evaluate the variation with time of the stress resulting from an initial temperature change. The material is assumed to be concrete with the same properties as defined in Example I, and the temperature change is applied 7 days after casting the concrete.

This example was used to investigate the effect on the results of different relaxation intervals in which the pseudo-loads are computed. Three different times were used, and the contours of the maximum compressive stress at 11 days are shown for each case in Fig. 36. The difference between 1/16 and 1/8 day computation interval appears quite slight.

A complete analysis was run using 1/8 day relaxation intervals with complete analyses every 2 days, for the period 7 to 21 days. The contours of minimum and maximum stress for the concrete at age 7 days and at 21 days are shown in Fig. 37, 38, 39 and 40. A comparison shows the great reduction in stress that occurs in this time, the changes are always smoothing and the areas of concentration almost relieved. Fig. 41 shows the principal stress trajectories for the time 7 days. The steady directions of the principal stress are apparent. Fig. 42 presents a three-dimensional section plot which shows the change of stress with time. This clearly shows that the most significant stress
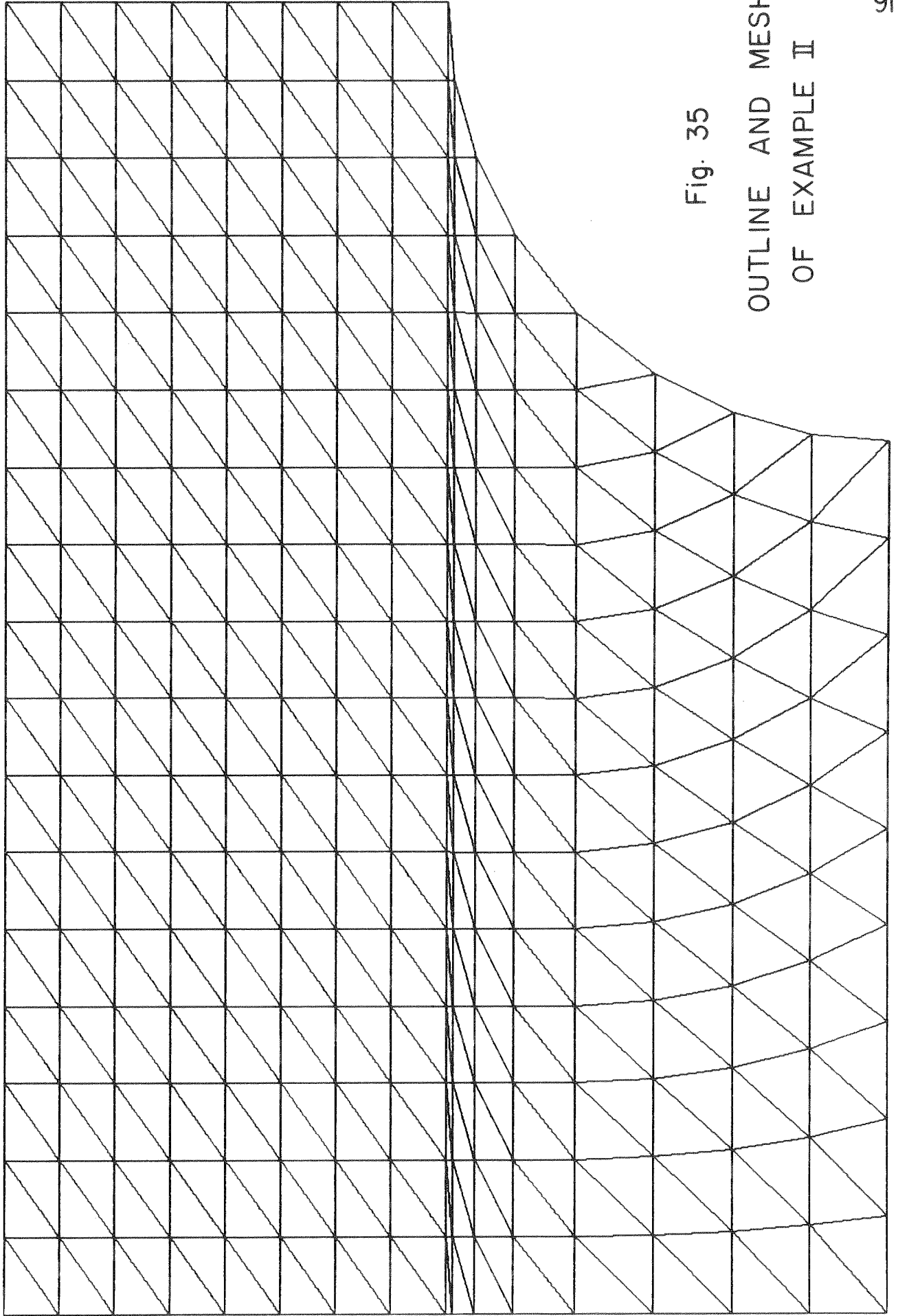
Fig. 35

OUTLINE AND MESH
OF EXAMPLE II

91

CONTOURS OF SIGMA MIN FOR DIFFERENT RELAXATION INTERVALS
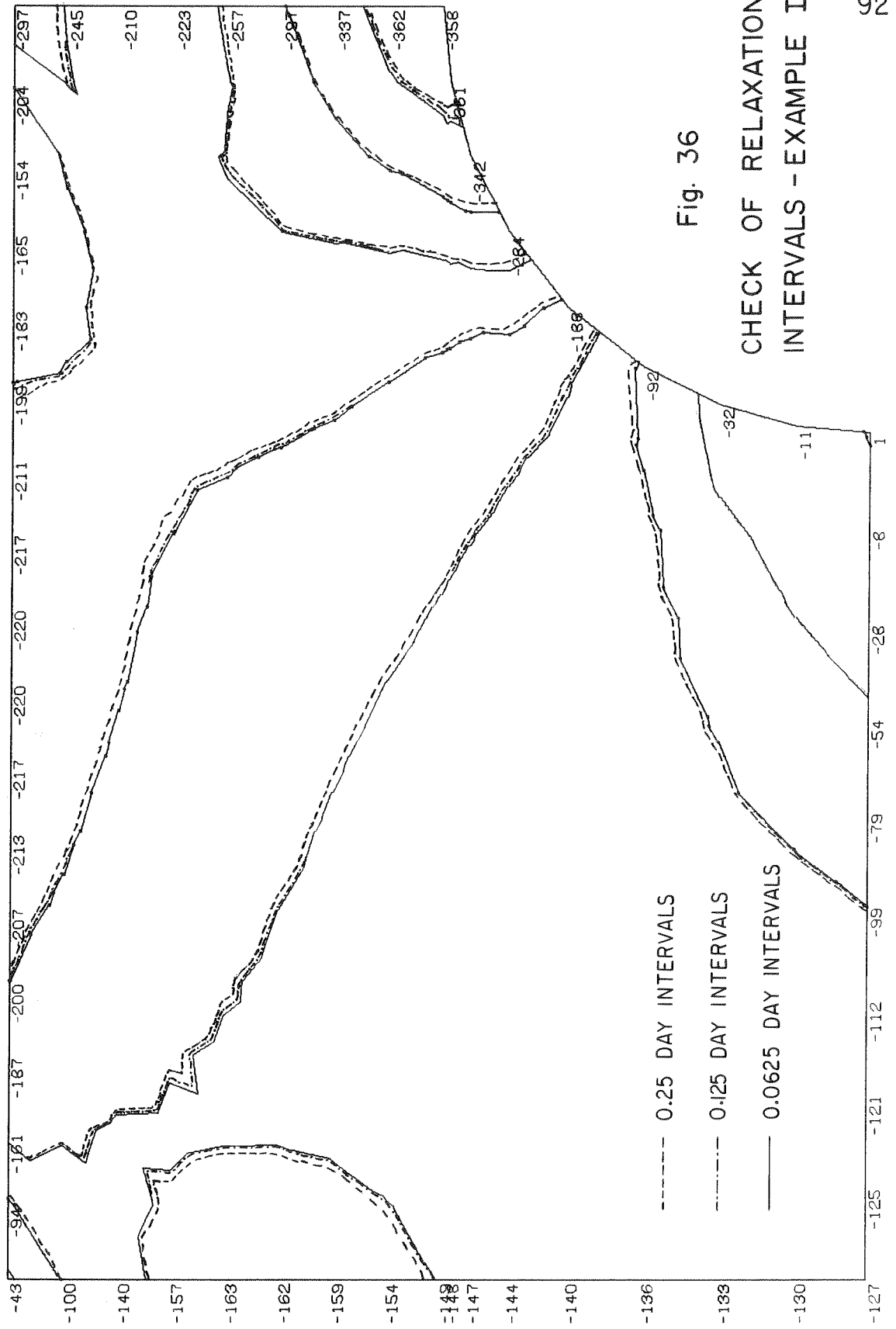
Fig. 36

CHECK OF RELAXATION
INTERVALS – EXAMPLE II

92

0.25 DAY INTERVALS

0.125 DAY INTERVALS

0.0625 DAY INTERVALS

CONTOURS OF SIGMA MIN AT 7 DAYS

Fig. 37

AUTOMATIC PLOTTER
RESULTS – EXAMPLE II

93

CONTOURS OF SIGMA MIN AT 21 DAYS
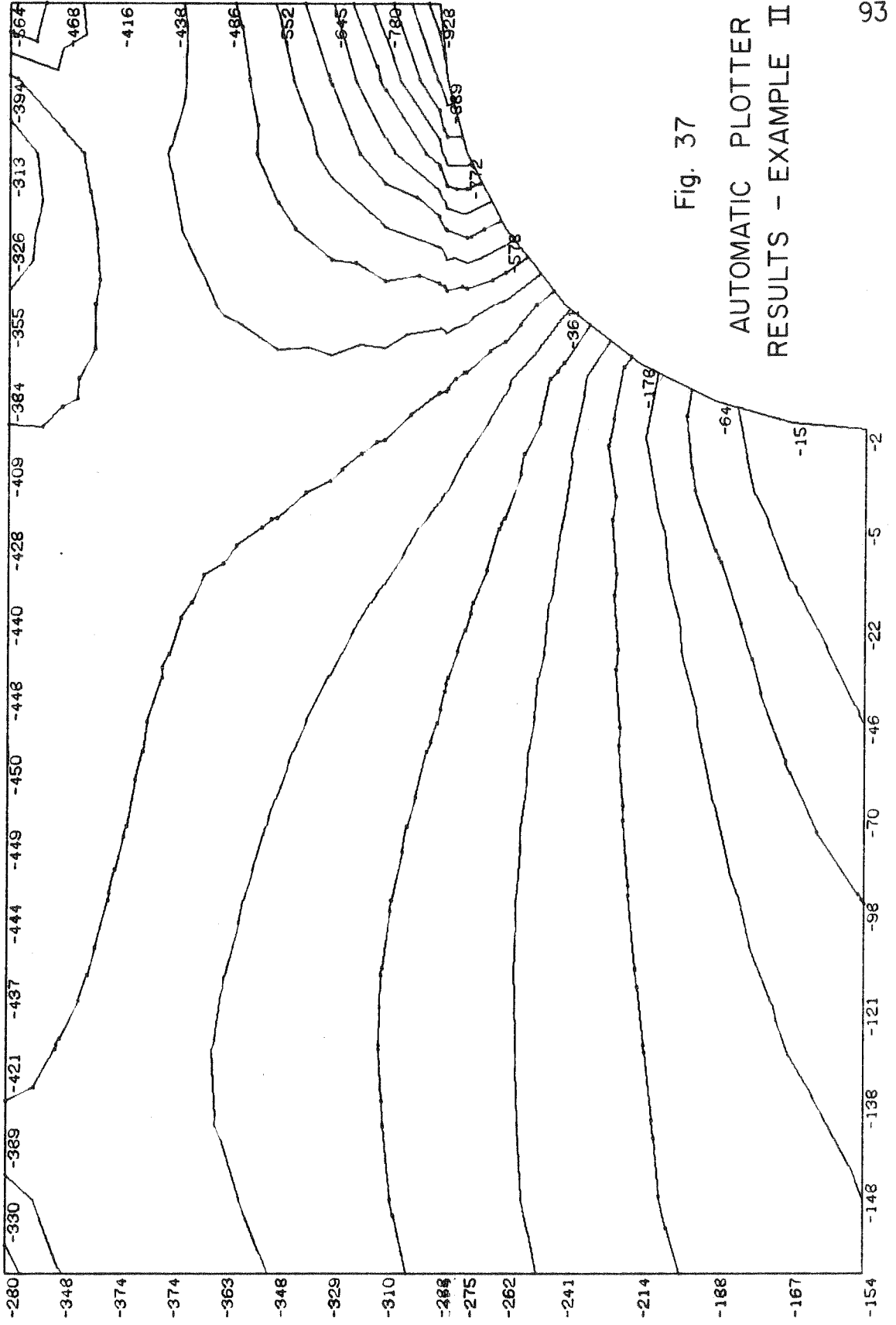

Fig. 38

AUTOMATIC PLOTTER
RESULTS — EXAMPLE II

94

CONTOURS OF SIGMA MAX AT 7 DAYS

Fig. 39

AUTOMATIC PLOTTER
RESULTS — EXAMPLE II

95

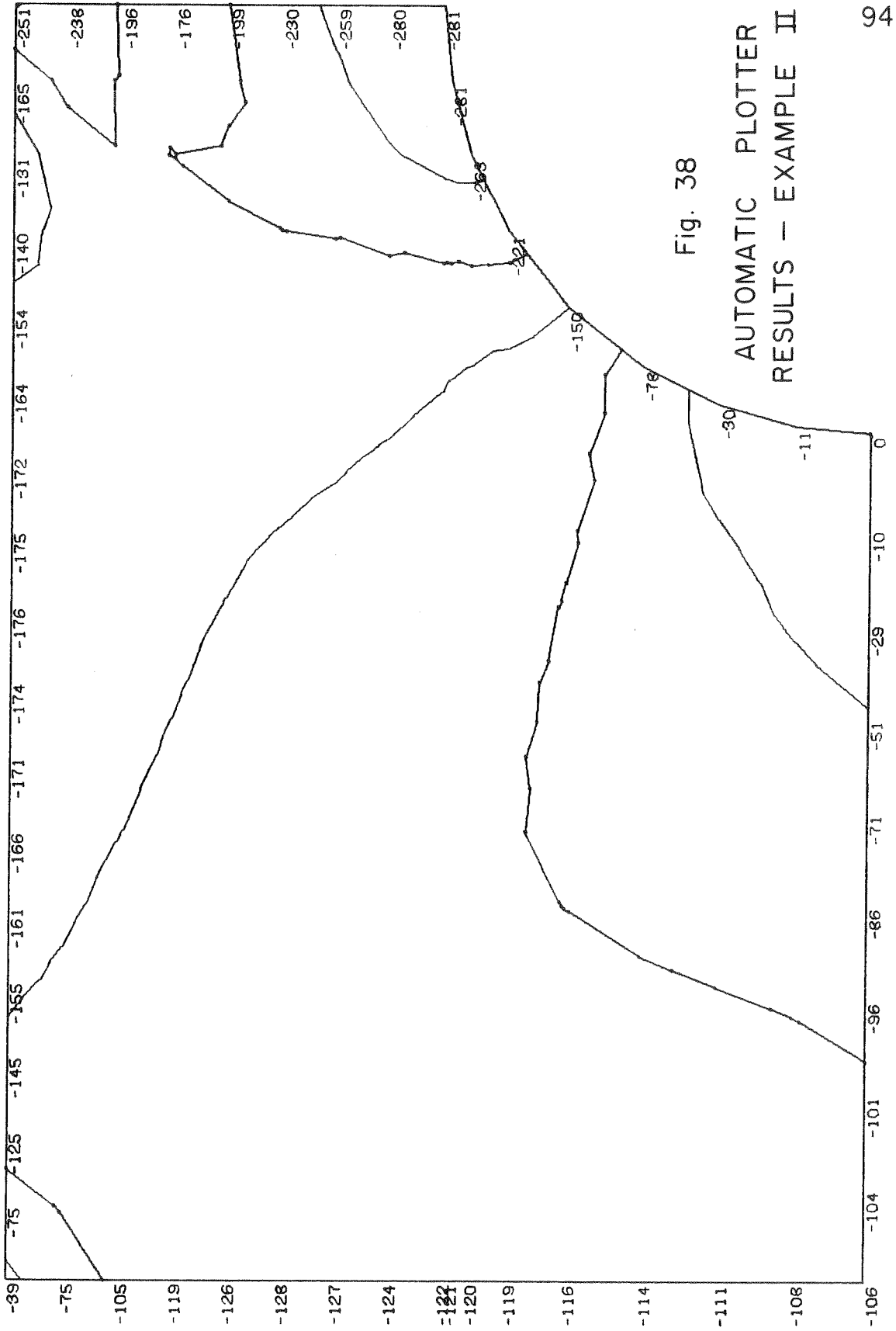CONTOURS OF SIGMA MAX AT 21 DAYS

Fig. 40

AUTOMATIC PLOTTER
RESULTS – EXAMPLE II

96

Fig. 41

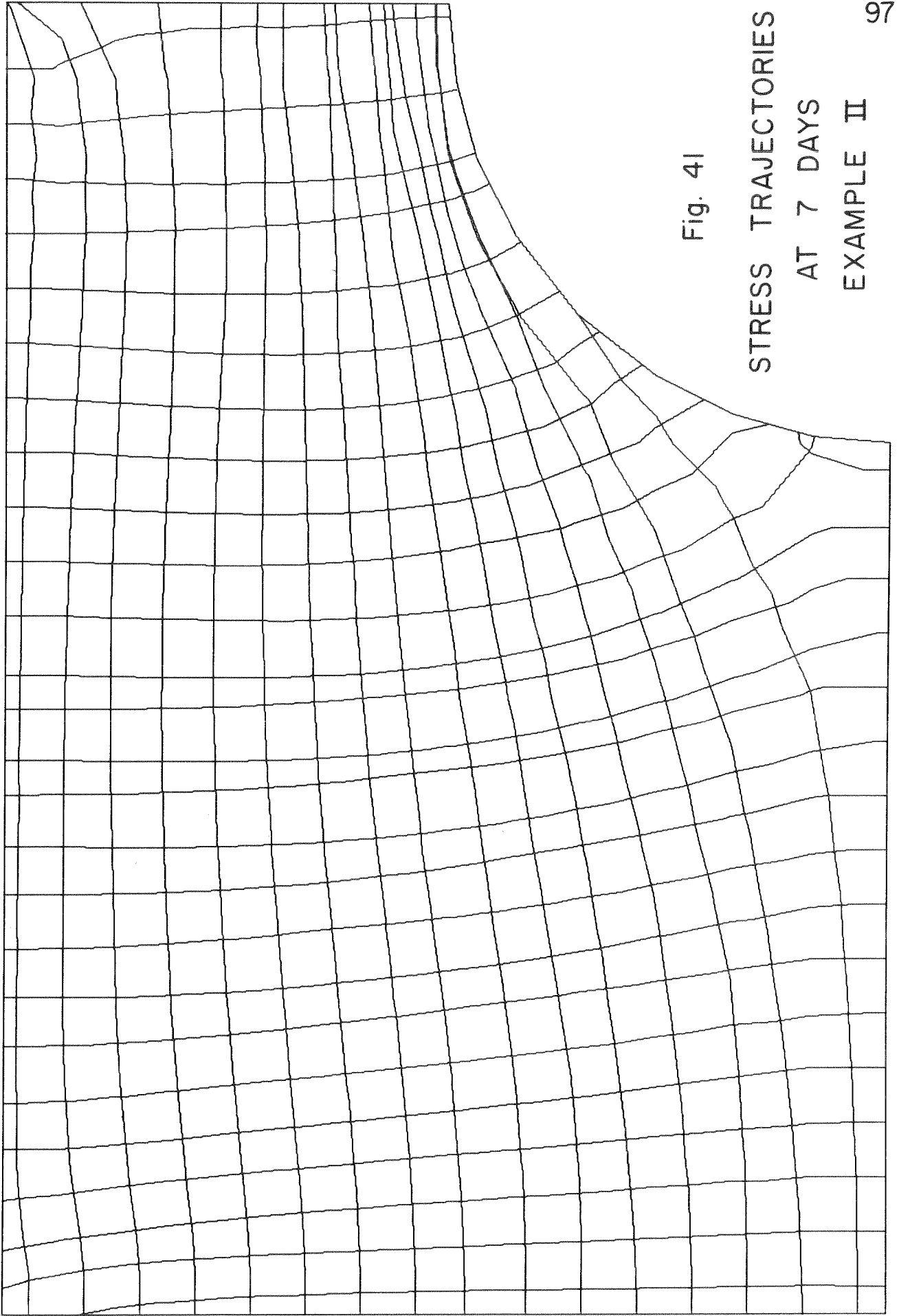STRESS TRAJECTORIES
AT 7 DAYS
EXAMPLE II

97

Fig. 42   VARIATION   OF   MINIMUM   STRESS   ACROSS   SECTION   AA   WITH   TIME

STRESS - PSI

40

30

20

10

0

TIME — DAYS

7 9 11 13 15 17 19 21

40

35

30

25

20

15

10

5

A

A

A

98
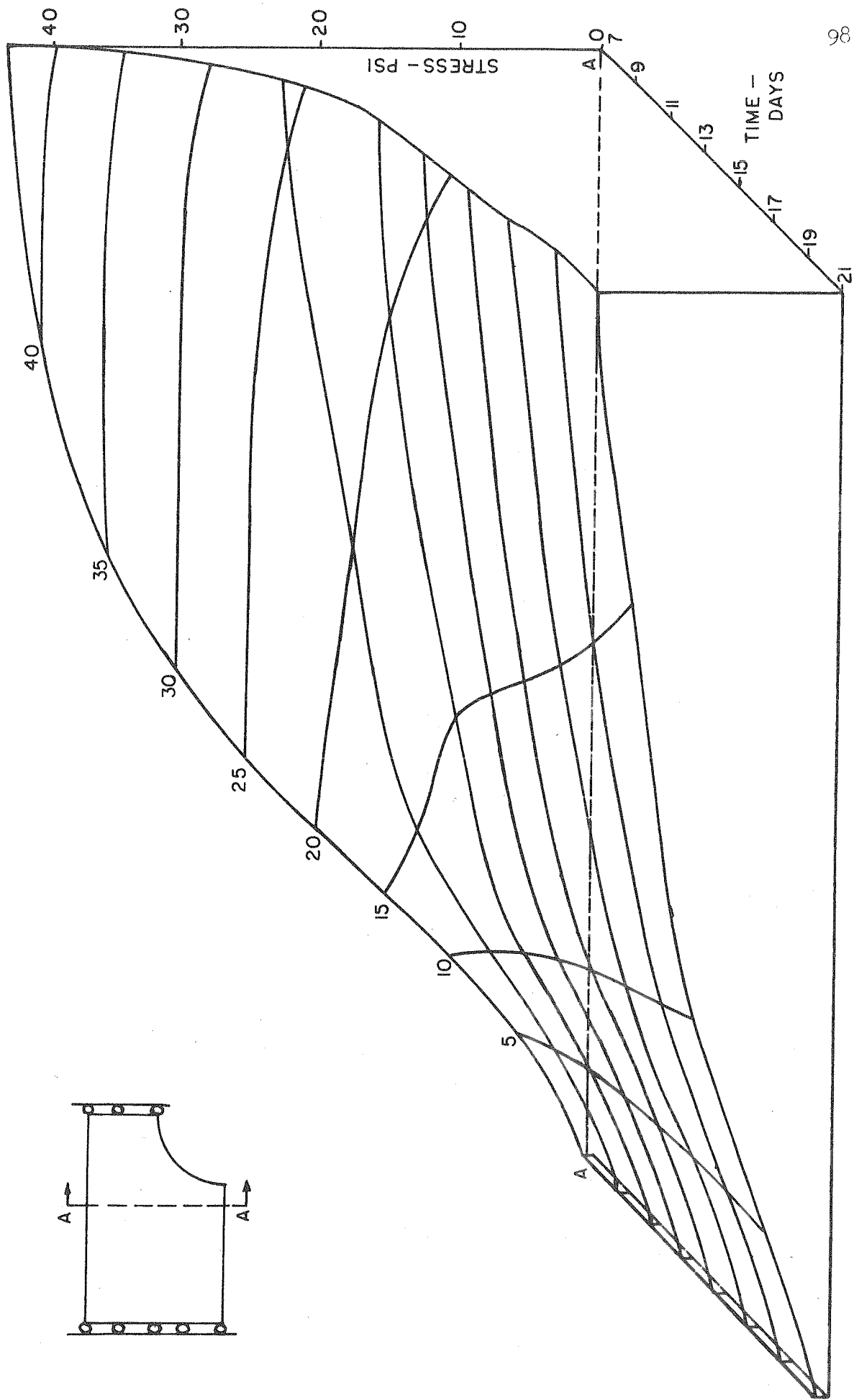
concentrations are quickly reduced and there is a tendency for a uniform stress to develop.

The automatic plotter was used to obtain Figs. 35-41 according to the procedures outlined in Chapter VIII. This example is a case where interpretation of results is quickly realized using such methods. The contours are of direct practical use to the engineer, and the trajectories give a feel of how the structure takes the loads.

X

CONCLUSIONS AND RECOMMENDATIONS

This dissertation has presented a feasible way of carrying out time dependent analyses of two-dimensional stress systems where the visco-elastic effect can be expressed in a Markov form. It is possible to express a wide range of creep data in this form by the use of Prony exponential series with enough terms.

The procedures of the computer program have been described and the results of two sample problems have shown that practical analyses can be obtained. The computer has also been utilized to compute triangular meshes automatically and plot the results, thus taking away much of the arduous labor associated with the previous use of finite element programs.

The generation of influence coefficients for an elastic foundation represents a first attempt to rationalize the problems of definition of boundary conditions for such structures as dams.

The direct solution procedures recently described[18] in connection with frame analysis are applicable to the problems in finite elements. In particular, for cases where the instantaneous elastic modulus can be considered a constant with respect to time, the solution time may be considerably shortened. In this case, the problem would be reduced to solving a repeated set of load conditions (pseudo-external loads) with the original stiffness matrix reduced to an upper triangular form. More than half of the computation would be eliminated.

The assumption associated with the expression of the one-dimensional test results into two dimensions is difficult to justify. However, if the directions of principal stress are approximately invariant, it would seem that this assumption is quite accurate.

The definition of creep in terms of the dilational and shear deformation gives a much more satisfactory basis for defining the variation is stress of a two dimensional element, but there is too little data available at this time to further investigate this approach.

There is considerable scope for the experimental worker in concrete to carry out tests which will make possible a more realistic analysis of two-dimensional systems. Such tests should be carried out on two and three dimensional systems where both creep and relaxation can occur.

With a more satisfactory definition of stresses over the complete system (the presently used stress-averaging method suggested by Wilson[6] does not give good results for stresses normal to a boundary line) the stress plotting routines may well come into their own in the interpretation of results.

XI

BIBLIOGRAPHY

1. Zienkiewicz, O.C., "The Stress Distribution in Gravity Dams,"
    Journal, Institution of Civil Engineers, Vol. 27,28, 1946, 1947.

2. Hrennikoff, A., "A Solution of Problems in Elasticity by the
    Framework Method," Transactions, The American Society of Mechan-
    ical Engineers, Vol. 8, No. 4, Dec., 1941.

3. McHenry, D., "A Lattice Analogy for Solution of Stress Problems,"
    Journal, Institute of Civil Engineers, Vol. 21-22, 1943-1944.

4. McCormick, C.W., "Plane Stress Analysis," Journal, Structural
    Division, A.S.C.E., Vol. 89, No. ST4, Aug., 1963.

5. Clough, R.W., "The Finite Element Method in Plane Stress Analysis,"
    Proceedings, A.S.C.E. 2nd Conference on Electronic Computation,
    Pittsburgh, Pennsylvania; Sept., 1960.

6. Wilson, E.L., "Finite Element Analysis of Two-Dimensional
    Structures," Doctoral Dissertation, Univ. of Calif., 1963.

7. Fraeijs de Veubeke, B., "Duality Between Displacement and Equili-
    brium Methods with a View to Obtaining Upper and Lower Bounds to
    Static Influence Coefficients," Proceedings, 14th Meeting of the
    AGARD Structures and Materials Panel, July, 1962.

8. Hanson, J.A., "A 10 Year Study of Creep Properties of Concrete,"
    U.S. Bureau of Reclamation Concrete Laboratory Report, S.P. 38,
    July, 1953.

9. McHenry, D., "A New Aspect of Creep in Concrete and its Application
    to Design," Proceedings, A.S.T.M., Vol. 43, 1943.

10. Hansen, T.C., "Creep and Stress Relaxation of Concrete,"
    Proceedings, Swedish Cement and Concrete Research Institute,
    Stockholm, 1960.

11. Duke, C.M., and Davis, H.E., "Some Properties of Concrete Under
    Sustained Combined Stresses," Proceedings, A.S.T.M., Vol. 44; 1944.

12. Ross, A.D., "Creep of Concrete under Variable Stress," Journal,
    American Concrete Institute, Vol. 29, March, 1958.

13. de Prony, R., "Essai Experimentale et Analytique," Journal, Ecole Polytech (Paris), Vol. 1, 1795.

14. Hildebrand, F.B., "Introduction to Numerical Analysis," Pages 378-382, McGraw-Hill, 1956.

15. Muskhelishvili, N.L., "Some Basic Problems of the Mathematical Theory of Elasticity," Pages 387-389, Noordhoff, 1953.

16. Schleicher, F., "Zur Theorie des Baugrundes," Der Bauingenieur, Vol. 7, 1926.

17. Clough, R.W., "The Stress Distribution of Norfork Dam," Institute of Engineering Research Report, Series 100, Issue 19, Berkeley, California; August, 1962.

18. Clough, R.W., Wilson, E.L., and King, I.P., "Large Capacity Frame Analysis Programs," Journal, Structural Division, A.S.C.E., Vol. 89, No. ST4; August, 1963.

ACKNOWLEDGEMENTS

The author would like to thank the following persons for their invaluable help in this study:

Professor J. M. Raphael, who as chairman of this thesis committee has kep direction to the research and made this final result possible.

Professor R. W. Clough, who guided the author through much of his research and was always willing to help with problems.

Professor D. H. Lehmer, who served on the thesis committee and advised on the mathematics.

Professor C. B. Brown, who served on the thesis committee and gave much practical assistance to the author.

And finally my wife, whose encouragement made this thesis a reality.

XIII

APPENDICES

APPENDIX I

APPLICATION OF NON-LINEAR CREEP EQUATION

The non-linear dependence of creep strain upon stress may be incorporated, if it is possible to express the equation in a Markov form and to assume that superposition of the individual increments may occur.

As an example, a single term exponential series will be used i.e., after m increments of stress

$$\epsilon_c = \sum_{i=1}^{m} \Delta \sigma_i^n \, a_1(t_i) \left\{ 1 - e^{-m(t-t_i)} \right\} \qquad \text{AI-1}$$

The right hand side must be expressible without need to summation each time. Then if

$$\sum^{m} \Delta \sigma_i^n \, a_1(t_i) = b_m \qquad \text{AI-2}$$

$$b_m = b_{m-1} + \Delta \sigma_m^n \, a_1(t_m) \qquad \text{AI-3}$$

and if

$$e^{-mt} \sum_{i=1}^{N} a_1(t_m) \Delta \sigma_i^n \, e^{mt_i} = e^{-mt} c_m \qquad \text{AI-4}$$

$$c_m = c_{m-1} + a_1(t_m) e^{mt_m} \Delta \sigma_m^n \qquad \text{AI-5}$$

The system is then in Markov form.

APPENDIX II

INTEGRATION OF EQUATION FOR HORIZONTAL DISPLACEMENTS

OF INFINITE HALF PLATE

$$u(x,y) = A \iint_{-a,-b}^{a,b} \frac{(x-\xi)}{(x-\xi)^2 + (y-\eta)^2} \, d\xi \, d\eta \qquad \text{where} \quad A = -\frac{(1-2\sigma)}{2(1-\sigma)} \frac{P}{\pi C}$$

$$= -\frac{A}{2} \int_{-b}^{+b} \left| \log_e \{(\xi-x)^2 + (\eta-y)^2\} \right|_{-a}^{+a} \, d\eta$$

$$= -\frac{A}{2} \int_{-b}^{b} \left[\log_e \{(a-x)^2 + (\eta-y)^2\} - \log_e \{(a+x)^2 + (\eta-y)^2\} \right] d\eta$$

Consider
$$I = \int \log(a^2 + x^2) \, dx$$

$$= x \log(a^2 + x^2) + 2a \tan^{-1} \frac{x}{a} - 2x$$

Then
$$u(x,y) = -\frac{A}{2} \left| (\eta-y) \log_e \left((a-x)^2 + (\eta-y)^2\right) + 2(a-x) \tan^{-1}\left(\frac{\eta-y}{a-x}\right) - 2(\eta-y) \right|_{-b}^{+b}$$

$$+ \text{term in } (a+x)$$

Thus
$$u(x,y) = \frac{1-2\sigma}{2(1-\sigma)} \frac{P}{\pi C} \left[(a-x) \tan^{-1}\left(\frac{b-y}{a-x}\right) + \frac{b-y}{2} \log_e \left((a-x)^2 + (b-y)^2\right) \right.$$

$$(a-x) \tan^{-1}\left(\frac{b+y}{a-x}\right) + \frac{b+y}{2} \log_e \left((a-x)^2 + (b+y)^2\right)$$

$$- (a+x) \tan^{-1}\left(\frac{b-y}{a+x}\right) + \frac{b-y}{2} \log_e \left((a+x)^2 + (b-y)^2\right)$$

$$\left. - (a+x) \tan^{-1}\left(\frac{b+y}{a+x}\right) + \frac{b+y}{2} \log_e \left((a+x)^2 + (b-y)^2\right) \right]$$